Statistical analysis of the effect of the symmetry energy on the crust-core transition density and pressure in neutron stars

Ilona Bednarek ©,* Jan Sładkowski ©,† and Jacek Syska ©‡

Institute of Physics, University of Silesia, 75 Pułku Piechoty 1, 41-500 Chorzów, Poland

Wiesław Olchawa ©§

Institute of Physics, University of Opole, Oleska 48, 45-052 Opole, Poland

There are generally two factors on which the form of the symmetry energy depends. The first one is the model involved in determining the nuclear matter equation of state, and the second the accuracy of the approximation of the symmetry energy function given by a Taylor series. Including the fourth-order term in the Taylor series accounts for a more reasonable representation of the symmetry energy. This paper focuses on understanding the symmetry energy influence on the neutron star crust-core phase boundary characteristics in terms of the above factors. All calculations were based on selected models of the relativistic mean field theory. The analysis begins with determining the analytical form of the fourth-order symmetry energy. The applied method allows for deriving the potential part of the fourth-order symmetry energy when the model contains various nonlinear couplings between mesons. The presence of the fourth-order term in the symmetry energy description affects the neutron star crust-core phase boundary characteristics by changing the transition density n_t, the corresponding pressure P_t, and the equilibrium proton fraction $Y_p^{\text{eq}}(n_t)$ value. The performed statistical analysis clarifies the role of the second- and fourth-order symmetry energy in determining the relationships between the transition density n_t and the leading coefficients characterizing the density dependence of the symmetry energy [$E_{\text{sym}}(n_0)$, L_{sym}, K_{sym}], where L_{sym} is the slope and K_{sym} is the curvature. It is shown that the regression analysis makes it possible to identify (P_t, L_{sym}, K_{sym}) as the group of factors that significantly influence the variability of the transition density n_t. The results also allow for estimating the effect of the fourth-order symmetry energy term inclusion. Additionally, the correlation analysis points to the individual role of L_{sym} and K_{sym}. Only when the fourth-order term is included are both variables K_{sym} and L_{sym} equally anticorrelated with n_t, leading to the increasing role of L_{sym} in analyzing the variability of n_t.

I. INTRODUCTION

Understanding the properties of dense nuclear matter is relevant for understanding not only nuclear physics experiments in the laboratory but also for building and testing theoretical models that describe and predict the behavior of neutron stars. The quality of the results depends on the accuracy with which theory can reproduce the energy density of nuclear matter and thus on how well the physics behind the model parameters can be controlled. The function describing energy density is generally calculated based on models of varying complexity [1–7]. It depends on the baryon number density $n_b = n_n + n_p$, where n_n and n_p are neutron and proton number densities, and the parameter $\delta = (n_n - n_p)/(n_n + n_p)$ describing the isospin asymmetry of the system. These two variables describe properties of the nuclear matter equation of state (EoS), which in terms of binding energy can be written as

$$E(n_b, \delta) = \frac{\varepsilon(n_b, \delta)}{n_b} - M, \tag{1}$$

where $\varepsilon(n_b, \delta)$ denotes the energy density and M is the nucleon mass. A convenient method of analyzing the EoS is decomposing it into the symmetric $E_0(n_b, 0)$ and isospin-dependent $E_{\text{asym}}(n_b, \delta)$ parts. Representing the function that describes the EoS by its Maclaurin series provides the possibility of separating the symmetric nuclear matter from that with isospin asymmetry. In such case, the EoS can be written as [8]

$$E(n_b, \delta) = E_0(n_b) + E_{\text{asym}}(n_b, \delta) = \sum_{n=0}^{\infty} E_{2n}(n_b)\delta^{2n}$$

$$= E_0(n_b) + E_{\text{sym},2}(n_b)\delta^2 + E_{\text{sym},4}(n_b)\delta^4 + \cdots. \tag{2}$$

This approximation is valid near $\delta = 0$. For finite nuclei, values of δ meet this condition, even in the parabolic approximation case [4,9]. Neutron stars offer an environment characterized by the extreme value of isospin asymmetry with a much larger value of δ, even close to unity. Thus, the

*ilona.bednarek@us.edu.pl
†jan.sladkowski@us.edu.pl
‡jacek.syska@us.edu.pl
§wolch@uni.opole.pl

TABLE I. Coefficients characterizing the density dependence of the nuclear matter EoS. Individual coefficients correspond to successive terms of the Taylor series expansion of the function given by Eq. (3).

$E_i(n_b)$	$k = 0$	$k = 1$	$k = 2$	$k = 3$
$E_0(n_b)$	$E_0(n_0)$	0	$K_0 = 9n_0^2 \frac{d^2 E_0(n_b)}{dn_b^2}\big|_{n_0}$	$J_0 = 27n_0^3 \frac{d^3 E_0(n_b)}{dn_b^3}\big|_{n_0}$
$E_{\mathrm{sym},2}(n_b)$	$E_{\mathrm{sym},2}(n_0)$	$L_2 = 3n_0 \frac{dE_{\mathrm{sym},2}(n_b)}{dn_b}\big|_{n_0}$	$K_{\mathrm{sym},2} = 9n_0^2 \frac{d^2 E_{\mathrm{sym},2}(n_b)}{dn_b^2}\big|_{n_0}$	$J_{\mathrm{sym},2} = 27n_0^3 \frac{d^3 E_{\mathrm{sym},2}(n_b)}{dn_b^3}\big|_{n_0}$
$E_{\mathrm{sym},4}(n_b)$	$E_{\mathrm{sym},4}(n_0)$	$L_4 = 3n_0 \frac{dE_{\mathrm{sym},4}(n_b)}{dn_b}\big|_{n_0}$	$K_{\mathrm{sym},4} = 9n_0^2 \frac{d^2 E_{\mathrm{sym},4}(n_b)}{dn_b^2}\big|_{n_0}$	$J_{\mathrm{sym},4} = 27n_0^3 \frac{d^3 E_{\mathrm{sym},4}(n_b)}{dn_b^3}\big|_{n_0}$

possibility that the parabolic approximation results will diverge cannot be excluded.

The usage of the higher-order terms is expected to provide a better approximation for the description of the isospin-dependent neutron star matter and neutron star properties, such as crust-core core transition density and the critical density for the direct Urca processes [10–16]. No experimental constraints exist on the fourth-order symmetry energy, even at the saturation density [17]. Unfortunately, different theoretical approaches predict $E_{\mathrm{sym},4}(n_0)$ values that vary significantly. Both nonrelativistic and relativistic mean field models (RMF) [18,19] and the approach based on chiral pion-nucleon dynamics [20] predict $E_{\mathrm{sym},4}(n_0)$ values less than 2 MeV. In the relativistic Hartree-Fock (RHF) approach, the values of the fourth-order symmetry energy $E_{\mathrm{sym},4}(n_b)$ are even lower than those obtained in RMF models for saturation density and densities more significant than n_0. The estimated $E_{\mathrm{sym},4}(n_0)$ values for selected RHF functionals are 0.35–0.58 MeV [21]. The performed quantum molecular dynamic (QMD) simulations of an isospin asymmetric system that contains neutrons, protons, and electrons leads to larger values of $E_{\mathrm{sym},4}(n_0)$. Depending on the parametrizations, they are 3.27, 7.07, 12.7 MeV [22].

It was found that the kinetic part of the isospin asymmetric EoS is significantly altered by correlated short-range nucleon pairs (SRCs) [23–25]. Considering such tensor force-induced SRC pairs, the kinetic part $E_{\mathrm{sym},2}^{\mathrm{kin}}(n_0)$ is reduced, and the part $E_{\mathrm{sym},4}^{\mathrm{kin}}(n_0)$ increases. The quartic term is predicted to be 7.18 ± 2.52 MeV [23] and differs significantly from the result obtained based on the free Fermi gas model (FFG), which gives the value of the kinetic part $E_{\mathrm{sym},4}^{\mathrm{kin}}(n_0) = 0.45$ MeV. A value as significant as 20.0 ± 4.6 MeV for the quartic term is estimated within an extended semiempirical nuclear mass formula based on analysis of finite nuclei fourth-order symmetry energy extracted from nuclear mass data [17]. The expansion coefficients of the series given by Eq. (2) depend on the density. The next step in analyzing the properties of nuclear matter is the Taylor series expansion of appropriate functions characterizing symmetric and asymmetric matter around the saturation point n_0:

$$E_i(n_b) = \sum_{k=0}^{\infty} (3n_0)^k \frac{1}{k!} \frac{d^k E_i(n_b)}{dn_b^k}\bigg|_{n_0} \left(\frac{n_b - n_0}{3n_0}\right)^k, \quad (3)$$

where for $i = 0$ the case of symmetric nuclear matter $E_0(n_b)$ is obtained, $i = 2$ corresponds to the second-order symmetry energy $E_{\mathrm{sym},2}(n_b)$, and $i = 4$ corresponds to the fourth-order symmetry energy $E_{\mathrm{sym},4}(n_b)$. Definitions of individual

coefficients in Eq. (3), corresponding to successive values of $E_i(n_b)$, are summarized in Table I.

Considering the case of SNM, the function $E_0(n_b)$ $(i = 0)$ expanded up to the third order in density is characterized by the following coefficients: $E_0(n_0)$, the binding energy per nucleon of SNM at saturation density n_0, the incompressibility coefficient K_0, and the skewness coefficient J_0:

$$E_0(n_b) = E_0(n_0) + \frac{K_0}{2!}\left(\frac{n_b - n_0}{3n_0}\right)^2$$
$$+ \frac{J_0}{3!}\left(\frac{n_b - n_0}{3n_0}\right)^3 + \cdots. \quad (4)$$

The function $E_{\mathrm{sym},2}(n_b)$ is represented by a series whose successive coefficients correspond to the value of the second-order symmetry energy at n_0, $E_{\mathrm{sym},2}(n_0)$, the symmetry energy slope parameter L_{sym}, and the curvature parameter $K_{\mathrm{sym},2}$. This method can be repeated for the next term in the considered equation. The function $E_{\mathrm{sym},4}(n_b)$ is approximated by the Taylor series with the following coefficients: the value of the fourth-order symmetry energy at n_0, $E_{\mathrm{sym},4}(n_0)$, the symmetry energy slope parameter $L_{\mathrm{sym},4}$, and the curvature parameter $K_{\mathrm{sym},4}$. Making the simplifying assumption of the Taylor series expansion, which retains only the leading order terms, satisfactorily represents the binding energy of nuclear matter; properties of this matter can be characterized by parameters, which are coefficients in this expansion. Constraints on the models of EoSs are obtained based on observables of two types: those that can be measured in terrestrial laboratories and those determined by astronomical observations. Accepted constraints are model dependent to varying degrees and enable EoS to be tested over different temperature, density, and isospin asymmetry ranges. Significant and still intensified experimental efforts are being undertaken to put the most reliable constraints on the properties of nuclear matter. The least uncertain limitations result from the properties of nuclei, namely nuclear masses and density distributions.

Laboratory experiments with heavy ion collisions (HIC) led to establishing a separate group of constraints. Variable experimental conditions, including beam energies, impact parameters, and the combination of the projectile and target nuclei, determine the usage of adequate observables. These factors allow one to study the properties of nuclear matter in different densities, temperatures, and isospin asymmetry ranges [26–28]. Focusing on the parameters characterizing the symmetry energy dependence on density, their experimental limitations, in addition to the mass measurements [29]

mentioned above, are mainly based on the measurements of neutron skin thickness [30–32], the polarizability of nuclear dipoles, the giant and pygmy resonance energies [33,34] of the dipoles flow in heavy ion collisions and isobaric analog states [35], isospin diffusion in heavy-ion reactions [36], isoscaling of fragments from intermediate energy heavy ion collisions [37], the frequency of isovector giant dipole resonances [38], and optical potentials from studying nucleon-nucleus scatterings [39,40]. There are many theoretical studies based on data from the PREX2 and CREX experiments that determined the parity-violating asymmetry A_{PV} in ^{48}Ca [41] and ^{208}Pb [30]. Nuclear models that allow inferring information on symmetry energy slope parameter L_{sym} based on these data lead to different results and put L_{sym} in the following ranges: $L_{\mathrm{sym}} = 106 \pm 37$ MeV [42] and $L_{\mathrm{sym}} = 53^{+14}_{-15}$ [43] MeV. The value $L_{\mathrm{sym}} = 54 \pm 8$ MeV was reported in the paper [44].

Some analyses try to explain the tension between the preferred values of L_{sym} by PREX-II and other experiments or observations [45]. A comprehensive analysis of correlations between the quantities of nuclear matter was carried out. The statistical analysis used in this paper included ordinary and partial, first- and second-order correlation coefficients, and multiple correlation coefficients. The correlations between the symmetry energy parameters were analyzed. The strength of the correlation between the dependent variables and (group of) factors used in regression models was calculated, and the overall statistical significance of these models was checked. To construct the hierarchy of the regression models for n_t vs P_t and groups of the symmetry energy parameters and to select the optimal model, type I and type II sums of squares (SS) were used. The stability of the estimators of the structural parameters of the regression models was checked using the variance inflation factor. The necessary information for the statistical analysis is included in the Appendix, which is quite sizable to avoid the common ambiguity of designations and terminology.

II. SYMMETRY ENERGY: FORMULAS AND A BRIEF OVERVIEW

A. The explicit form of the fourth-order symmetry energy term

The starting point for deriving the explicit forms of the second- and fourth-order symmetry energy, and thus carrying out a more in-depth analysis of properties of asymmetric nuclear matter, is selecting the Lagrange density function. Its general form $\mathcal{L}$, making detailed reference to the system dynamic, considers nucleons and mesons as degrees of freedom and can be written as

$$
\begin{aligned}
\mathcal{L} = & \bar{\psi}\big[\gamma^{\mu}\big(i\partial_{\mu} + g_{\omega}\omega_{\mu} + g_{\rho}\tau^{a}\rho_{\mu}^{a}\big) - (M - g_{\sigma}\sigma)\big]\psi \\
& + \tfrac{1}{2}\partial^{\mu}\sigma\,\partial_{\mu}\sigma - \tfrac{1}{4}F^{\mu\nu}F_{\mu\nu} - \tfrac{1}{4}B^{a}_{\mu\nu}B^{\mu\nu a} \\
& + U_M(\sigma, \omega, \rho),
\end{aligned} \tag{5}
$$

where ψ denotes the nucleon field, σ, ω_{μ}, ρ_{μ}^{a} are the scalar, vector, and vector-isovector meson fields, respectively, M is the nucleon mass, and τ^{a} denotes Pauli matrices. $F_{\mu\nu}$ and $B^{a}_{\mu\nu}$

are the vector field tensors:

$$
\begin{aligned}
F_{\mu\nu} &= \partial_{\mu}\omega_{\nu} - \partial_{\nu}\omega_{\mu}, \\
B^{a}_{\mu\nu} &= \partial_{\mu}\rho_{\nu}^{a} - \partial_{\nu}\rho_{\mu}^{a} - g_{\rho}\varepsilon^{abc}\rho_{\mu}^{b}\rho_{\nu}^{c}.
\end{aligned}
$$

The function $U_M(\sigma, \omega, \rho)$ includes the meson mass terms and different types of meson self- and mixed-interaction couplings. All calculations performed in this paper and the qualitative conclusions drawn neglect the effects beyond the applied mean field approximation. In this approach, a meson field is split into the constant classical component and the component resulting from quantum fluctuations, which vanish after taking its vacuum expectation value. As a result, only the classical components remain:

$$
\begin{aligned}
\sigma &\to \langle\sigma\rangle \equiv s, \\
\omega^{\mu} &\to \langle\omega\rangle \equiv \langle\omega_0\rangle\delta^{\mu 0} \equiv \omega_0, \\
\bar{\rho}^{\mu} &\to \langle\rho_3\rangle \equiv \langle\rho_{0,3}\rangle\delta^{\mu 0} \equiv r_{0,3}.
\end{aligned} \tag{6}
$$

Calculations that allow one to determine the analytical form of the second- and fourth-order symmetry energy are based on the method and notation presented in [46], and are carried out generally without specification of the potential function U_M. The presented method, in the case of a system composed of nucleons and mesons, uses a function representing the energy density written as a sum of the following components:

$$
\begin{aligned}
\varepsilon = & \sum_{j=n,p} \varepsilon_j^{\mathrm{kin}}(n_b, \delta, s) + U_M(s, \omega_0, r_{0,3}) \\
& + g_{\omega}\omega_0 n_b + \frac{1}{2}g_{\rho}r_{0,3}n_{3b} \\
= & \sum_{j=n,p} \varepsilon_j^{\mathrm{kin}}(n_b, \delta, s) + U_M(s, \omega_0, r_{0,3}) \\
& + g_{\omega}\omega_0 n_b - \frac{1}{2}g_{\rho}r_{0,3}n_b\delta.
\end{aligned} \tag{7}
$$

The baryon number density $n_b = n_n + n_p$ is calculated with the use of the relation

$$
n_j = \int_0^{k_{Fj}} \frac{d^3k}{(2\pi)^3} = \frac{1}{3\pi^2}k_{Fj}^3, \tag{8}
$$

$j = n, p$, and $n_{3b} = \langle\bar{\psi}\gamma^0\tau_3\psi\rangle = n_p - n_n = -n_b\delta$. The kinetic energy contribution takes the form

$$
\begin{aligned}
\varepsilon_j^{\mathrm{kin}} &= \frac{1}{\pi^2}\int_0^{k_{Fj}} k^2\sqrt{k^2 + M_{\mathrm{eff}}^2}\,dk \\
&= \frac{1}{4}\left\{\frac{1}{\pi^2}E_{Fj}k_{Fj}^3 + M_{\mathrm{eff}}\,\rho_{Sj}(n_b, \delta, s)\right\},
\end{aligned} \tag{9}
$$

where the scalar density $\rho_S = \langle\bar{\psi}\psi\rangle = \rho_{Sn} + \rho_{Sp}$, defined as

$$
\begin{aligned}
\rho_{Sj} &= -\frac{1}{g_{\sigma}}\frac{\partial\varepsilon_j^{\mathrm{kin}}}{\partial s} = \frac{M_{\mathrm{eff}}}{2\pi^2}\left\{k_{Fj}E_{Fj} - M_{\mathrm{eff}}^2\ln\frac{k_{Fj} + E_{Fj}}{M_{\mathrm{eff}}}\right\} \\
&(j = n, p),
\end{aligned} \tag{10}
$$

depends on the effective nucleon mass $M_{\mathrm{eff}} \equiv M_{\mathrm{eff}}(s) = M - g_{\sigma}s$ and on the energy $E_{Fj} = \sqrt{k_{Fj}^2 + M_{\mathrm{eff}}^2}$. Meson fields are functions that depend on two independent variables n_b and δ,

i.e., $s(n_b, \delta)$, $\omega_0(n_b, \delta)$, and $r_{0,3}(n_b, \delta)$. Still, this is not explicitly stated in the above formulas for simplicity of notation. Equations of motion resulting from the condition

$$\frac{\partial \varepsilon}{\partial \phi_i} = 0 \quad \text{for } \phi_i = s, \omega_0, r_{0,3} \tag{11}$$

have to be satisfied for any n_b and δ values and can be written in the following form:

$$-g_\sigma \, \rho_S(n_b, \delta, s) + \frac{\partial U_M(s, \omega_0, r_{0,3})}{\partial s} = 0,$$

$$g_\omega n_b + \frac{\partial U_M(s, \omega_0, r_{0,3})}{\partial \omega_0} = 0, \tag{12}$$

$$-\frac{1}{2} g_\rho n_b \delta + \frac{\partial U_M(s, \omega_0, r_{0,3})}{\partial r_{0,3}} = 0.$$

Following the procedure described in [46], differentiating the equations of motion with respect to n_b, the system of linear equations for the derivatives of meson fields can be obtained. These equations can be written succinctly in a matrix form:

$$\hat{m}_{\text{eff}}^2 \frac{d\hat{\Phi}}{dn_b}\bigg|_{\delta \text{ fixed}} = -\hat{g}, \tag{13}$$

where the effective mass matrix is defined by

$$m_{\phi_i\phi_j,\text{eff}}^2 = \frac{\partial^2 \varepsilon}{\partial \phi_i \partial \phi_j} \quad \text{for } \phi_i = \phi_j = s \text{ or } \phi_i \neq \phi_j, \tag{14}$$

$$m_{\phi_i\phi_i,\text{eff}}^2 = -\frac{\partial^2 \varepsilon}{\partial \phi_i^2} \quad \text{for } \phi_i = \omega_0, r_{0,3}, \tag{15}$$

and $\hat{\Phi} = (s, \omega_0, r_{0,3})^T$. Based on Eq. (12), the explicit form of the matrix $\hat{m}_{\text{eff}}^2$ is as follows:

$$\hat{m}_{\text{eff}}^2 \equiv \begin{pmatrix} m_{\sigma,\text{eff}}^2 & m_{\sigma\omega,\text{eff}}^2 & m_{\sigma\rho,\text{eff}}^2 \\ m_{\sigma\omega,\text{eff}}^2 & -m_{\omega,\text{eff}}^2 & m_{\omega\rho,\text{eff}}^2 \\ m_{\sigma\rho,\text{eff}}^2 & m_{\omega\rho,\text{eff}}^2 & -m_{\rho,\text{eff}}^2 \end{pmatrix}$$

$$= \begin{pmatrix} \frac{\partial^2 U_M}{\partial s^2} - g_\sigma \frac{\partial \rho_S}{\partial s} & \frac{\partial^2 U_M}{\partial s \partial \omega} & \frac{\partial^2 U_M}{\partial s \partial r_{0,3}} \\ \frac{\partial^2 U_M}{\partial s \partial \omega} & \frac{\partial^2 U_M}{\partial \omega^2} & \frac{\partial^2 U_M}{\partial \omega \partial r_{0,3}} \\ \frac{\partial^2 U_M}{\partial s \partial r_{0,3}} & \frac{\partial^2 U_M}{\partial \omega \partial r_{0,3}} & \frac{\partial^2 U_M}{\partial r_{0,3}^2} \end{pmatrix}, \tag{16}$$

with the column matrix $\hat{g}$,

$$\hat{g} \equiv \left(-g_\sigma \frac{\partial \rho_S}{\partial n_b}, \; g_\omega, \; -g_\rho \delta/2 \right)^T$$

$$= \left(-\frac{g_\sigma M_{\text{eff}}}{2} \left[\frac{1}{E_{Fp}} + \frac{1}{E_{Fn}} \right], \; g_\omega, \; -g_\rho \delta/2 \right)^T. \tag{17}$$

Differentiating the equations of motion (12) with respect to the variable δ, the following expression can be derived:

$$\hat{m}_{\text{eff}}^2 \frac{d\hat{\Phi}}{d\delta}\bigg|_{n_b \text{ fixed}} = -\tilde{g}, \tag{18}$$

where

$$\tilde{g} \equiv \left(-g_\sigma \frac{\partial \rho_S}{\partial \delta}, \; 0, \; -g_\rho n_b/2 \right)^T$$

$$= \left(-\frac{g_\sigma M_{\text{eff}}}{2} \left[\frac{1}{E_{Fp}} - \frac{1}{E_{Fn}} \right], \; 0, \; -g_\rho n_b/2 \right)^T. \tag{19}$$

The particular case of symmetric nuclear matter is considered separately. The nonzero value of the variable δ is the measure of the deviation from this state of matter, so $\delta = 0$ corresponds to symmetric matter. In this case, the fields become functions of one variable, $s(n_b, 0)$, $\omega_0(n_b, 0)$, and $r_{0,3}(n_b, 0)$, and the system of equations of motion takes the form

$$-g_\sigma \, \rho_S(n_b, 0, s) + \frac{\partial U_M(s, \omega_0, r_{0,3})}{\partial s} = 0,$$

$$g_\omega n_b + \frac{\partial U_M(s, \omega_0, r_{0,3})}{\partial \omega_0} = 0, \tag{20}$$

$$\frac{\partial U_M(s, \omega_0, r_{0,3})}{\partial r_{0,3}} = 0.$$

The solution $r_{0,3}(n_b, 0) \equiv 0$ can be obtained from the last equation of the system given by Eq. (20), under reasonable assumptions about the form of the U_M potential. The expectation value of the ρ meson field is generally an order of magnitude smaller than that of the ω field, so higher-order nonlinear couplings of the ρ meson are not considered as they have only a marginal influence on the properties of finite nuclei and neutron stars. Taking the solution $r_{0,3}(n_b, 0) = 0$, the first two equations of Eq. (20) form a nonlinear system of equations for the unknowns $s(n_b, 0)$ and $\omega_0(n_b, 0)$. It is assumed that the function describing the potential has the following properties:

$$\frac{\partial^2 U_M}{\partial s \partial r_{0,3}}\bigg|_{\delta=0} = \frac{\partial^2 U_M}{\partial \omega_0 \partial r_{0,3}}\bigg|_{\delta=0} = 0. \tag{21}$$

In the following considerations, the symbol Q (e.g., $Q_{\sigma\omega} \equiv m_{\sigma\omega,\text{eff}}^2$) as the symbol of effective meson masses is adopted. This simplifies the notation and emphasizes that these effective masses correspond to symmetric matter (cf. [18]). According to the general procedure given by the formulas (18) and (19) one can obtain

$$\hat{Q} \frac{d\hat{\Phi}}{d\delta}\bigg|_{\delta=0} = 0, \quad -Q_\rho \frac{dr_{0,3}}{d\delta}\bigg|_{\delta=0} = \frac{1}{2} g_\rho n_b, \tag{22}$$

where

$$\hat{Q} \equiv \begin{pmatrix} Q_\sigma & Q_{\sigma\omega} \\ Q_{\sigma\omega} & -Q_\omega \end{pmatrix}$$

$$= \begin{pmatrix} \left(\frac{\partial^2 U_M}{\partial s^2} - g_\sigma \frac{\partial \rho_S}{\partial s} \right)\big|_{\delta=0} & \frac{\partial^2 U_M}{\partial s \partial \omega}\big|_{\delta=0} \\ \frac{\partial^2 U_M}{\partial s \partial \omega}\big|_{\delta=0} & \frac{\partial^2 U_M}{\partial \omega^2}\big|_{\delta=0} \end{pmatrix}, \tag{23}$$

$$Q_\rho = -\frac{\partial^2 U_M}{\partial r_{0,3}^2}\bigg|_{\delta=0}, \quad \Phi = (s, \omega_0)^T. \tag{24}$$

Solutions of Eq. (22) are

$$\frac{d\hat{\Phi}}{d\delta}\bigg|_{\delta=0} = (0, 0)^T, \quad \frac{dr_{0,3}}{d\delta}\bigg|_{\delta=0} = -\frac{g_\rho n_b}{2Q_\rho} \tag{25}$$

The next step in the calculations is to determine the second derivatives of the fields:

$$\frac{d^2\hat{\Phi}}{d\delta^2}\bigg|_{\delta=0} = -n_b \hat{Q}^{-1}\hat{G}, \quad \frac{d^2 r_{0,3}}{d\delta^2}\bigg|_{\delta=0} = 0, \tag{26}$$

where

$$
\hat{Q}^{-1} = \frac{1}{1+x}\begin{pmatrix} 1/Q_\sigma & x/Q_{\sigma\omega} \\ x/Q_{\sigma\omega} & -1/Q_\omega \end{pmatrix}, \quad x \equiv \frac{Q_{\sigma\omega}^2}{Q_\sigma Q_\omega}, \quad (27)
$$

$$
\hat{G} = (G_\sigma, G_\omega)^T
$$

$$
= \left(-\frac{g_\sigma}{n_b}\frac{\partial^2 \rho_S}{\partial \delta^2}\bigg|_{\delta=0} + \frac{1}{n_b}\frac{\partial^3 U_M}{\partial s\,\partial^2 r_{0,3}}\left(\frac{dr_{0,3}}{d\delta}\right)^2\bigg|_{\delta=0}, \right.
$$

$$
\left. \frac{1}{n_b}\frac{\partial^3 U_M}{\partial \omega_0\,\partial^2 r_{0,3}}\left(\frac{dr_{0,3}}{d\delta}\right)^2\bigg|_{\delta=0} \right)^T. \quad (28)
$$

So the solutions are as follows:

$$
\frac{d^2 s}{d\delta^2}\bigg|_{\delta=0} = -\frac{n_b}{1+x}\left(\frac{G_\sigma}{Q_\sigma} + x\frac{G_\omega}{Q_{\sigma\omega}}\right),
$$

$$
\frac{d^2\omega}{d\delta^2}\bigg|_{\delta=0} = -\frac{n_b}{1+x}\left(x\frac{G_\sigma}{Q_{\sigma\omega}} - \frac{G_\omega}{Q_\omega}\right). \quad (29)
$$

The performed calculations are the basis for determining the symmetry energy. Note that for all values of n_b and δ the following relation holds:

$$
\frac{d\varepsilon}{d\delta} = \frac{\partial \varepsilon}{\partial \delta} = \frac{\partial\left(\varepsilon_n^{\mathrm{kin}} + \varepsilon_p^{\mathrm{kin}}\right)}{\partial \delta} - \frac{1}{2}g_\rho n_b\, r_{0,3}(n_b,\delta). \quad (30)
$$

Therefore, one can write

$$
E_{\mathrm{sym},2}(n_b) = \frac{1}{2}\frac{d^2}{d\delta^2}\left(\frac{\varepsilon}{n_b} - M\right)\bigg|_{\delta=0} = \frac{1}{2n_b}\frac{d^2\varepsilon}{d\delta^2}\bigg|_{\delta=0}
$$

$$
= \frac{1}{2n_b}\frac{d}{d\delta}\frac{\partial\left(\varepsilon_n^{\mathrm{kin}} + \varepsilon_p^{\mathrm{kin}}\right)}{\partial \delta}\bigg|_{\delta=0} - \frac{g_\rho}{4}\frac{dr_{0,3}}{d\delta}\bigg|_{\delta=0}
$$

$$
= \frac{k_F^2}{6E_F} + \frac{g_\rho^2 n_b}{8Q_\rho}. \quad (31)
$$

Similarly

$$
E_{\mathrm{sym},4}(n_b) = \frac{1}{24n_b}\frac{d^3}{d\delta^3}\frac{\partial\left(\varepsilon_n^{\mathrm{kin}} + \varepsilon_p^{\mathrm{kin}}\right)}{\partial \delta}\bigg|_{\delta=0} - \frac{g_\rho}{48}\frac{d^3 r_{0,3}}{d\delta^3}\bigg|_{\delta=0}
$$

$$
= \frac{1}{24n_b}\left\{\frac{\partial^4\left(\varepsilon_n^{\mathrm{kin}} + \varepsilon_p^{\mathrm{kin}}\right)}{\partial \delta^4} - 3g_\sigma \frac{\partial^2 \rho_S}{\partial \delta^2}\frac{d^2 s}{d\delta^2}\right\}\bigg|_{\delta=0}
$$

$$
+ \frac{1}{8n_b}\left(\frac{dr_{0,3}}{d\delta}\right)^2\left\{\frac{\partial^3 U_M}{\partial s\,\partial^2 r_{0,3}}\frac{d^2 s}{d\delta^2}\right.
$$

$$
+ \left.\frac{\partial^3 U_M}{\partial \omega_0\,\partial^2 r_{0,3}}\frac{d^2\omega_0}{d\delta^2}\right\}\bigg|_{\delta=0}
$$

$$
+ \frac{1}{8}\left\{G_\sigma\frac{d^2 s}{d\delta^2} + G_\omega\frac{d^2\omega_0}{d\delta^2}\right\}\bigg|_{\delta=0}. \quad (32)
$$

Finally, after some algebra,

$$
E_{\mathrm{sym},4}(n_b) = \frac{k_F^2}{648E_F^5}\left(10k_F^4 + 4M_{\mathrm{eff}}^4 + 11k_F^2 M_{\mathrm{eff}}^2\right)
$$

$$
- \frac{n_b}{8(1+x)}\left(\frac{G_\sigma^2}{Q_\sigma} - \frac{G_\omega^2}{Q_\omega} + 2x\frac{G_\sigma G_\omega}{Q_{\sigma\omega}}\right). \quad (33)
$$

B. The case of the explicit form of the meson potential

The performed calculations were based on relativistic mean-field (RMF) models. This approach describes the nuclear many-body problem as a relativistic system of baryons and mesons. The original Walecka model determines properties of nuclear matter by the scalar-isoscalar σ (attractive) and vector-isoscalar ω mesons (repulsive) exchange [47,48]. This model was extended by including the vector-isovector ρ meson and then underwent further modifications that increased its applicability. Much more sophisticated models have a variety of nonlinear meson interaction [49] terms that allow for their classification according to types of nonlinear meson couplings [50,51].

Determination of the properties of nuclear matter in the case of RMF models is based on selected groups of parameters, which are the subject of the research reported in papers [51,52]. The justification for choosing these parametrizations is based on the compliance of the calculated properties of nuclear matter with different values of isospin asymmetry with the limitations resulting from the analysis of experimental data. Considering the isospin-dependent nuclear matter [53], the experimental constraints refer to the coefficients characterizing the symmetry energy dependence on density. The following ranges of constraints can be specified: for the symmetry energy coefficient $E_{\mathrm{sym}}(n_0)$, 25–35 and 30–35 MeV [54]; for the symmetry energy slope L_0 evaluated at n_0, 25–115 MeV [55,56]; for the volume part of the isospin incompressibility $K_{\tau,v}^0$ at n_0, -700 to -400 MeV [51,57,58]; and for the ratio of the symmetry energy at $n_0/2$ to its value at n_0, 0.57–0.86 [59].

Analysis of the nuclear matter EoS, especially its high-density limit, carried out based on the relativistic mean field approach and taking into account different types of nonlinear couplings between mesons has been presented in [60]. In paper [60], the coupling constants $g_\sigma, g_\omega, g_\rho$ together with the parameters that define the strength of the meson nonlinear interactions are determined by imposing a set of constraints which includes the nuclear saturation density $n_0 = 0.153 \pm 0.005$ fm^{-3} [61]; the binding energy per nucleon $E_0(n_0) = -16.1 \pm 0.2$ MeV [51]; incompressibility $K_0 = 230 \pm 40$ MeV [62,63]; the symmetry energy at the nuclear saturation density $E_{\mathrm{sym}}(n_0) = 32.5 \pm 1.8$ MeV [64]; the pressure of pure neutron matter (PNM) determined at the densities 0.08, 0.12, and 0.16 fm^{-3} from a chiral effective field theory (χEFT) calculation [65], with $2 \times$ N^{3}LO (next-to-next-to-next-to leading order) uncertainty in the likelihood, the pressure of PNM being an increasing function of density $dP/dn_b > 0$; and in the case of neutron star models the maximum mass is required to be above two solar masses [66].

The models used in this paper are also distinguishable by different types of nonlinear couplings between mesons. It becomes possible to divide all the models into three groups. Group I includes BSR models [67] and FSUGZ03, FSUGZ06 [68] with the following types of the mixed meson couplings: σ-ω^2, σ^2-ω^2, σ-ρ^2, σ^2-ρ^2, ω^2-ρ^2. Group II of BKA models [69], G2 [70], and G2* [71] comprises σ-ω^2, σ^2-ω^2, σ-ρ^2 nonlinear terms. Group III of FSUGold [62],

FSUGold4 [72], IU FSU, XS [73], and TM1 [74] is characterized by ω^2-ρ^2 coupling. Parameter values for individual models are gathered in the paper [75]. In general, the function

U_M can contain a variety of self and mixed meson couplings. For the aims of this paper, it is convenient to write it in the form

$$U_M(s, \omega, r_{0,3}) = \frac{1}{2}m_\sigma^2 s^2 + \frac{A}{3}s^3 + \frac{B}{4}s^4 - \frac{1}{2}m_\omega^2\omega_0^2 - \frac{C}{4}\left(g_\omega^2\omega_0^2\right)^2 - \frac{1}{2}m_\rho^2 r_{0,3}^2$$
$$-g_\sigma s\,(g_\omega\omega_0)^2\left(\alpha_1 + \frac{1}{2}\alpha_1' g_\sigma s\right) - g_\sigma s\,(g_\rho r_{0,3})^2\left(\alpha_2 + \frac{1}{2}\alpha_2' g_\sigma s\right) - \frac{1}{2}\alpha_3'(g_\omega\omega_0)^2(g_\rho r_{0,3})^2. \tag{34}$$

Taking the form of the potential given by Eq. (34), the following equations of motion were obtained:

$$m_\sigma^2 s + As^2 + Bs^3 - g_\sigma(\alpha_1 + \alpha_1' g_\sigma s)(g_\omega\omega_0)^2 - g_\sigma(\alpha_2 + \alpha_2' g_\sigma s)(g_\rho r_{0,3})^2 = g_\sigma\,\rho_S,$$
$$m_\omega^2\omega_0 + g_\omega[C(g_\omega\omega_0)^3 + (2\alpha_1 + \alpha_1' g_\sigma s)g_\sigma s g_\omega\omega_0] = g_\omega\,n_b, \tag{35}$$
$$m_\rho^2 r_{0,3} + g_\rho[(2\alpha_2 + g_\sigma\alpha_2' s)g_\sigma s g_\rho r_{0,3} + \alpha_3'(g_\omega\omega_0)^2 g_\rho r_{0,3}] = -g_\rho\,n_b\,\delta.$$

Knowing the energy density of the system, the second- and the fourth-order symmetry energy can be determined based on Eqs. (31) and (33). The individual components expressing the explicit form of the second- and fourth-order symmetry energy, in the case of the selected potential function given by Eq. (34), can be rewritten as

$$G_\sigma = -(\alpha_2 + g_\sigma\alpha_2' s)\frac{g_\sigma g_\rho^4 n_b}{2Q_\rho^2} + \frac{1}{3}\frac{g_\sigma k_F^2 M_{\text{eff}}}{E_F^3}, \tag{36}$$

$$G_\omega = -\frac{\alpha_3' g_\rho^4 g_\omega^2 \omega_0 n_b}{2Q_\rho^2}. \tag{37}$$

The effective meson masses that enter Eqs. (31) and (33) now have the forms

$$Q_\rho = m_\rho^2 + (2\alpha_2 + g_\sigma\alpha_2' s)g_\rho^2 g_\sigma s + g_\rho^2\alpha_3'(g_\omega\omega_0)^2, \tag{38}$$

$$Q_\sigma = m_\sigma^2 + 2As + 3Bs^2 - \alpha_1' g_\sigma^2(g_\omega\omega_0)^2 + 3g_\sigma^2\left(\frac{\rho_S}{M_{\text{eff}}} - \frac{n_b}{E_F}\right), \tag{39}$$

$$Q_\omega = m_\omega^2 + (2\alpha_1 + g_\sigma\alpha_1' s)g_\omega^2 g_\sigma s + 3Cg_\omega^4\omega_0^2, \tag{40}$$

$$Q_{\sigma\omega} = 2(\alpha_1 + g_\sigma\alpha_1' s)g_\sigma g_\omega^2\omega_., \tag{41}$$

In the above expressions, Eqs. (36)–(41), all the fields are calculated for $\delta = 0$ (symmetric nuclear matter). Under the assumption that all coupling constants except α_3' equal zero, a simplified form of the potential is obtained:

$$U_M(s, \omega, r_{0,3}) = \frac{1}{2}m_\sigma^2 s^2 + \frac{A}{3}s^3 + \frac{B}{4}s^4 - \frac{1}{2}m_\omega^2\omega_0^2 - \frac{C}{4}(g_\omega^2\omega_0^2)^2 - \frac{1}{2}m_\rho^2 r_{0,3}^2 - \frac{1}{2}\alpha_3'(g_\omega\omega_0)^2(g_\rho r_{0,3})^2. \tag{42}$$

In this case, calculations performed for the fourth-order symmetry energy reproduce the result obtained by Cai *et al.* [18].

III. SYMMETRY ENERGY AGAINST CHANGES IN A NEUTRON STAR CRUST-CORE TRANSITION DENSITY AND PRESSURE

The existing studies conclude that the parameters of nuclear matter are, to varying degrees, correlated with each other and with the characteristics of nuclei and neutron stars. A thorough analysis of the symmetry energy and especially the quality of its approximation by Taylor series requires an understanding of the necessity of including the fourth-order term in the Taylor expansion, particularly in the case of nuclear matter with a significant value of isospin asymmetry. Only after that does the checking of the symmetry energy effect on specific physical quantities become more credible.

The results of terrestrial experiments point to impressive progress in finding constraints on the nuclear matter EoS. Simultaneously, the corresponding improvement also addresses astrophysical observations, which, applied to determining neutron star parameters, can lead to additional complementary constraints. However, an attempt to answer the question about the dependence of symmetry energy on density based on information obtained from observations of neutron stars is still subject to considerable uncertainty.

A separate issue is an analysis and systematics of neutron star properties to identify those that explicitly depend on the form of the symmetry energy. One of the essential characteristics of this type is the location of the edge of a neutron star core, which corresponds to the phase transition from the homogeneous matter in the core to the inhomogeneous matter at low densities in the crust.

The questionable point in constructing a neutron star model is the precise determination of a region in a neutron star

interior where the crust-core phase boundary occurs. In this context, the additional limitations on the crust-core transition density and pressure obtained using the existing experimental and theoretical constraints on the coefficients describing the symmetry energy cannot be overestimated. Thus, the density region relevant for the core-crust transition in neutron stars offers the possibility to analyze the symmetry energy effect on neutron star structure.

Several approaches have been developed to evaluate the value of the transition density. These include the dynamic method, the thermodynamic method, and the random phase approximation. The method of determining the density for which liquid-gas instability appears is widely applicable both for finite temperature, focusing in this case on the dynamics of supernovae, as well as considering the limiting case of zero temperature when describing neutron star crust [76–79]. The thermodynamic method of assessing the transition density used in this paper consists of determining such a value of the density at which the instability caused by small amplitude density fluctuations in a homogeneous liquid begins to develop, indicating the beginning of the formation of a nuclear cluster [80–83]. Accordingly, it is indispensable for the system to meet the conditions of mechanical and chemical stability to ensure that any local density fluctuations will not diverge. The following inequalities express these conditions:

$$-\left(\frac{\partial P}{\partial v}\right)_\mu > 0, \qquad -\left(\frac{\partial \mu_{\text{asym}}}{\partial q_c}\right)_v > 0, \qquad (43)$$

where v and q_c are volume and charge per baryon number, P is the total pressure of the system, and $\mu_{\text{asym}} = \mu_n - \mu_p$ is the difference of neutron and proton chemical potentials. The second condition is usually satisfied, whereas the first one leads to the requirement of positivity of the expression

$$V_{\text{ther}} = 2n_b \frac{\partial E(n_b, Y_p)}{\partial n_b} + n_b^2 \frac{\partial^2 E(n_b, Y_p)}{\partial n_b^2}$$
$$- \left(n_b \frac{\partial^2 E(n_b, Y_p)}{\partial n_b \partial Y_p}\right)^2 \Big/ \frac{\partial^2 E(n_b, Y_p)}{\partial Y_p^2}, \qquad (44)$$

where $E(n_b, Y_p)$ is the binding energy, and $Y_p = (1-\delta)/2$. The chemical composition of neutron star matter is settled by conditions of the charge neutrality and the β equilibrium, which determines the relationship between the chemical potentials of the constituents of the matter, and results in the implicit-like equation for the isospin asymmetry of the system

$$\mu_{\text{asym}} \equiv \mu_n - \mu_p = \mu_e, \qquad (45)$$

where μ_e is the electron chemical potential. Assuming that the relation

$$E(n_b, Y_p) = E_{\text{sym},2}(n_b)(1-2Y_p)^2 + E_{\text{sym},4}(n_b)(1-2Y_p)^4$$
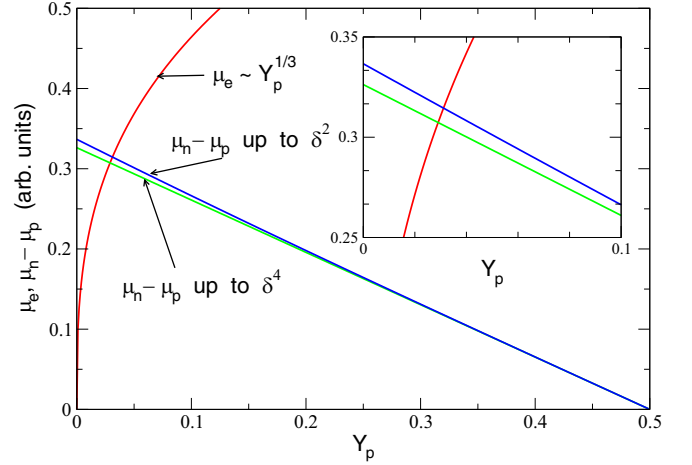
FIG. 1. This figure illustrates, for the chosen density, the influence of the fourth-order symmetry energy term on the solution of the equation defining the equilibrium concentration of protons.

can approximate the isospin-dependent part of the energy per nucleon of nuclear matter, the electron chemical potential μ_e can be given by

$$\mu_e = \mu_n - \mu_p = -\frac{\partial E(n_b, Y_p)}{\partial Y_p}$$
$$= 4(1-2Y_p)E_{\text{sym},2}(n_b) + 8(1-2Y_p)^3 E_{\text{sym},4}(n_b). \quad (46)$$

In the case of relativistic electrons, their chemical potential is of the form

$$\mu_e = \hbar c (3\pi^2 n_b)^{1/3} Y_e^{1/3}. \qquad (47)$$

The charge neutrality condition $Y_p(n_b) = Y_e(n_b)$ can be used to derive the equation determining the equilibrium proton fraction Y_p^{eq}:

$$\hbar c (3\pi^2 n_b)^{1/3} Y_p^{1/3} = 4(1-2Y_p)E_{\text{sym},2}(n_b)$$
$$+ 8(1-2Y_p)^3 E_{\text{sym},4}(n_b) \qquad (48)$$

for a given baryon number n_b.

The symmetry energy is the decisive factor determining the protons' equilibrium concentration. The approximate analytical form of the solution of Eq.(48) can be obtained when the symmetry energy is determined in the parabolic approximation. Including the symmetry energy fourth-order term blurs the seemingly easy parabolic form of the obtained equilibrium proton fraction. The influence of the symmetry energy fourth-order term on the equilibrium concentration of protons is illustrated in Fig. 1 by comparing the left and right sides of Eq. (48). Determining the transition density value comes down to solving the equation $V_{\text{ther}} = 0$ while considering the conditions of charge neutrality and β equilibrium. Assuming that the energy in the isospin-dependent sector includes contributions from the fourth-order symmetry energy term, Eq. (49) takes the form

$$V_{\text{ther}} = n_b^2 \left[\frac{d^2 E_0(n_b)}{dn_b^2} + (1-2Y_p)^2 \left(\frac{d^2 E_{\text{sym},2}(n_b)}{dn_b^2} + (1-2Y_p)^2 \frac{d^2 E_{\text{sym},4}(n_b)}{dn_b^2}\right)\right]$$

$$+ 2n_b \left[\frac{dE_0(n_b)}{n_b} + (1 - 2Y_p)^2 \left(\frac{dE_{\text{sym},2}(n_b)}{dn_b} + (1 - 2Y_p)^2 \frac{dE_{\text{sym},4}(n_b)}{dn_b} \right) \right]$$

$$- 2n_b^2 (1 - 2Y_p)^2 (E_{\text{sym},2}(n_b) + 6(1 - 2Y_p)^2 E_{\text{sym},4}(n_b))^{-1} \left(\frac{dE_{\text{sym},2}(n_b)}{dn_b} + 2(1 - 2Y_p)^2 \frac{dE_{\text{sym},4}(n_b)}{dn_b} \right)^2. \quad (49)$$

The total pressure P needed to support the considered npe system is supplied by the contributions of nucleons (P_N) and electrons (P_e), $P = P_N + P_e$. Using the thermodynamic relation the following equation for the pressure at the crust-core transition density n_t and equilibrium proton fraction $Y_t \equiv Y_p^{\text{eq}}(n_t)$ can be obtained:

$$P(n_t) = n_t^2 \left. \frac{dE_0(n_b)}{dn_b} \right|_{n_t} + n_t^2 (1 - 2Y_t)^2 \left(\left. \frac{dE_{\text{sym},2}(n_b)}{dn_b} \right|_{n_t} + (1 - 2Y_t)^2 \left. \frac{dE_{\text{sym},4}(n_b)}{dn_b} \right|_{n_t} \right)$$

$$+ n_t Y_t (1 - 2Y_t) [E_{\text{sym},2}(n_t) + 2E_{\text{sym},4}(n_t)(1 - 2Y_t)^2]. \quad (50)$$

The values of n_t and P_t have been obtained based on numerical solution of Eqs. (48)–(50) without applying the expansion of $E_{\text{sym},2}(n_b)$ and $E_{\text{sym},4}(n_b)$ around n_0.

It is instructive to compare the effects of the symmetry energy function approximations. Two methods of approximations that lead to different representations of the symmetry energy can be used for this purpose. The first uses the parabolic approximation for the Taylor series expansion around $\delta = 0$. As a result, the function $E_{\text{sym},2}(n_b)$ is obtained, which subsequently is expanded around n_0 up to the fourth order. In the second approach, the expansion around $\delta = 0$ is additionally supplied by a fourth-order term $E_{\text{sym},4}(n_b)$. Calculating the transition density n_t, equilibrium proton fraction Y_t, and transition pressure P_t following Eqs. (48), (49), and (50) includes contributions from both functions $E_{\text{sym},2}(n_b)$ and $E_{\text{sym},4}(n_b)$. The functions $E_{\text{sym},2}(n_b)$ and $E_{\text{sym},4}(n_b)$ are then also expanded up to the fourth order around n_0. The presented approaches were used to calculate Y_t, n_t, and P_t. The calculations were carried out for the selected BRS8 parametrization. The obtained results show differences between the two approximations and also in comparison to the values obtained by numerically solving Eqs. (48) and (49) without applying the expansion of $E_{\text{sym},2}(nb)$ and $E_{\text{sym},4}(nb)$ around n_0. Similarly, the pressure P_t was calculated by inserting into the formula (50) these numerical values of Y_t and n_t together with functions $E_{\text{sym},2}(n_b)$ and $E_{\text{sym},4}(n_b)$ for which the approximation in the form of expansion around n_0 was not applied. The obtained results are presented for the parabolic approximation and the case when the fourth-order term is included (the expansion around δ) in the following order: the numerically calculated value and then terms that refer to the expansions around n_0 to the fourth, third, and second order, respectively:

$$n_{t2} = (0.0780, 0.0724, 0.0653, 0.0583),$$
$$n_{t24} = (0.0767, 0.0710, 0.0646, 0.0584),$$
$$Y_{t2} = (0.0290, 0.0281, 0.0276, 0.0277),$$
$$Y_{t24} = (0.0309, 0.0279, 0.0275, 0.0277),$$
$$P_{t2} = (0.2922, 0.2120, 0.1288, 0.0868),$$
$$P_{t24} = (0.2999, 0.2178, 0.1407, 0.1041). \quad (51)$$

n_{t2} and n_{t24} are given in fm^{-3} whereas P_{t2} and P_{t24} in MeV/fm^3. The inclusion of the higher-order terms in the description of the symmetry energy has also been applied to analyze the uncertainties in neutron star properties by applying the Bayesian approach [60,84].

This paper aims to show the impact of including the fourth-order term in δ to describe the symmetry energy function. This is justified when we analyze the properties of nuclear matter with a high value of isospin asymmetry. In this case, the limitation to the parabolic approximation may give results inconsistent with exact values, especially significant for transition pressure P_t. Properties of the neutron star crust-core phase boundary such as the transition density n_t, corresponding pressure P_t, and equilibrium proton fraction Y_t calculated for the considered models are given in Table II.

IV. RESULTS

A. Effect of the symmetry energy on the core-crust phase boundary in neutron stars

Before a more detailed analysis of the fourth-order symmetry energy $E_{\text{sym},4}(n_b)$ applicability is provided, it is worth comparing the density dependence of the $E_{\text{sym},2}(n_b)$ and $E_{\text{sym},4}(n_b)$ functions calculated for the considered groups of models. The results, presented in Fig. 2, show that the symmetry energy is an increasing function of the density for each parametrization. Individual cases differ in the slope L_{sym} and the rate of increase, which is reflected in the value of the K_{sym} coefficient. The density dependence of $E_{\text{sym},4}(n_b)$ has a more complex form given by Eq. (33). Defining the function, which represents the second term of Eq. (33), the potential part of the fourth-order symmetry energy can be identified:

$$E_{\text{sym},4}^{\text{pot}}(n_b) = -\frac{n_b}{8(1 + x)} \left(\frac{G_\sigma^2}{Q_\sigma} - \frac{G_\omega^2}{Q_\omega} + 2x \frac{G_\sigma G_\omega}{Q_{\sigma\omega}} \right). \quad (52)$$

Figure 3 shows a series of figures that visualize the function defined by Eq. (52). A common feature of plots presented in this figure is a sequence of local minima and maxima, which differ in values for individual parametrizations. The function $E_{\text{sym},4}^{\text{pot}}(n_b)$ assumes the highest values at maxima and deeper minima for models in group III. Differences between the results obtained for individual models reveal themselves

TABLE II. Properties of the neutron star crust-core phase boundary [the transition density n_t, corresponding pressure P_t, and equilibrium proton fraction $Y_p^{eq}(n_t)$] are calculated when the parabolic approximation gives the symmetry energy and when the fourth-order term is also included. The subscript 2 refers to the quantities calculated based on the parabolic approximation, and the subscript 24 indicates the sum of the second and fourth-order contributions.

Model	n_{t2} (fm^{-3})	$Y_p^{eq}(n_{t2})$	P_{t2} (MeV/fm^3)	n_{t24} (fm^{-3})	$Y_p^{eq}(n_{t24})$	P_{t24} (MeV/fm^3)
BSR8	0.0777	0.0290	0.2922	0.0767	0.03086	0.2999
BSR9	0.0777	0.0285	0.3394	0.0765	0.0304	0.3424
BSR10	0.0778	0.0284	0.4390	0.0760	0.0300	0.4284
BSR11	0.0794	0.0282	0.5679	0.0769	0.0295	0.5344
BSR12	0.0849	0.0305	0.7219	0.0821	0.0318	0.6758
BSR15	0.0754	0.0273	0.2725	0.0744	0.0292	0.2784
BSR16	0.0761	0.0279	0.3033	0.0750	0.0297	0.3070
BSR17	0.0775	0.0275	0.4016	0.0759	0.0291	0.3929
BSR18	0.0799	0.0279	0.5362	0.0777	0.0294	0.5104
BSR19	0.0830	0.0286	0.6952	0.0800	0.0298	0.6434
BSR20	0.0833	0.0280	0.7778	0.0796	0.0369	0.6988
FSUGZ03	0.0778	0.0283	0.3431	0.0766	0.0301	0.3456
FSUGZ06	0.0763	0.0276	0.3072	0.0751	0.0295	0.3103
BKA20	0.0804	0.0260	0.4941	0.0783	0.0274	0.4704
BKA22	0.0776	0.0263	0.4958	0.0752	0.0276	0.4687
BKA24	0.0796	0.0273	0.6235	0.0766	0.0283	0.5743
G2	0.0866	0.0277	0.9251	0.0817	0.0277	0.8004
G2*	0.0812	0.0210	0.4677	0.0794	0.0222	0.4387
FSUGold	0.0865	0.0336	0.5286	0.0858	0.0369	0.5506
FSUGold4	0.0827	0.0347	0.2721	0.0830	0.0393	0.3125
XS	0.0776	0.0335	0.1829	0.0773	0.0379	0.2069
TM1	0.0947	0.0347	0.6455	0.0939	0.0379	0.6718
IU-FSU	0.0902	0.0368	0.2577	0.0915	0.0425	0.3169

in quantities Q_σ, Q_ω, Q_ρ, and $Q_{\omega\sigma}$ that define $E_{sym,4}^{pot}(n_b)$. Table III summarizes their detailed forms. These quantities, considered in terms of effective meson masses and the G_σ and G_ω factors given by Eq. (28), affect the range and strength of interactions between the mesons. The reader should consider that, in general, the matrix of effective masses [Eq. (16)] is not diagonal, and its terms do not necessarily correspond to physical masses. Another item distinguishing the third group

is the vanishing of the factor x. Its form for groups I and II is shown in Fig. 4. The complete form of the fourth-order symmetry energy is presented in Fig. 5. A noticeable modification through the potential part occurs only in the case of models belonging to the third group. Comparing Figs. 3 and 5, it is evident that the kinetic part of the symmetry energy prevails over the potential one. The exceptions are models of group III, for which the kinetic and potential parts are of comparable

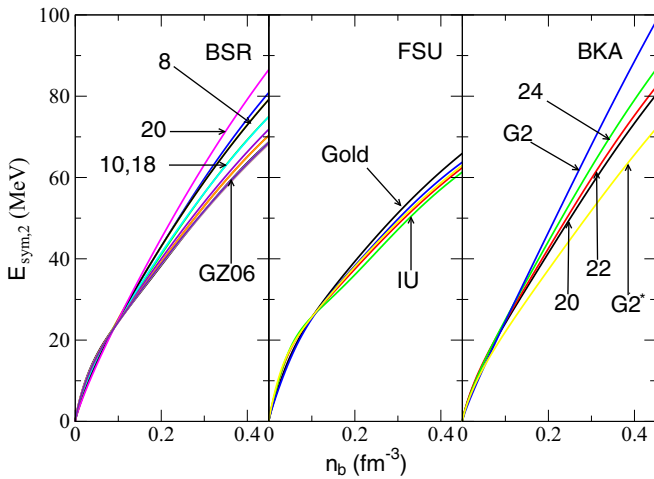FIG. 2. The dependence on the density of the symmetry energy $E_{sym,2}$, obtained in the case of the parabolic approximation for three distinguished groups of models.
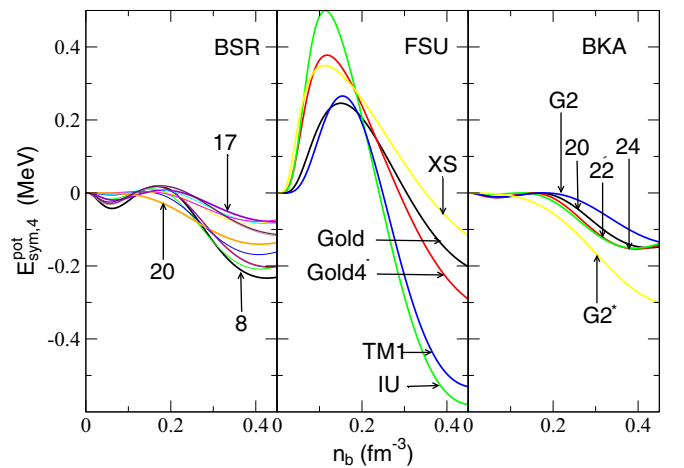

FIG. 3. Density dependence of the fourth-order symmetry energy potential part. The results obtained for the three distinguished groups of models point to the third group as the one having the most significant contribution of the potential part.

TABLE III. Factors characterizing the potential part of the fourth-order symmetry energy $E_{\text{sym,4}}$. $Q_{i,0}$, where $(i = \sigma, \omega)$, denotes the part of the quantity Q_i that does not contain mixed-mesons coupling terms. In the case of ρ meson, $Q_{\rho,0} \equiv m_\rho^2$.

Model	Group I	Group II	Group III
Q_σ	$Q_{\sigma,0} - \alpha_1' g_\sigma^2 (g_\omega \omega_0)^2$	$Q_{\sigma,0} - \alpha_1' g_\sigma^2 (g_\omega \omega_0)^2$	$Q_{\sigma,0}$
Q_ω	$Q_{\omega,0} + (2\alpha_1 + g_\sigma \alpha_1' s) g_\omega^2 g_\sigma s$	$Q_{\omega,0} + (2\alpha_1 + g_\sigma \alpha_1' s) g_\omega^2 g_\sigma s$	$Q_{\omega,0}$
Q_ρ	$Q_{\rho,0} + (2\alpha_2 + g_\sigma \alpha_2' s) g_\rho^2 g_\sigma s + g_\rho^2 \alpha_3' (g_\omega \omega_0)^2$	$Q_{\rho,0} + 2\alpha_2 g_\rho^2 g_\sigma s$	$Q_{\rho,0} + g_\rho^2 \alpha_3' (g_\omega \omega_0)^2$
$Q_{\omega\sigma}$	$2(\alpha_1 + g_\sigma \alpha_1' s) g_\sigma g_\omega^2 \omega_0$	$2(\alpha_1 + g_\sigma \alpha_1' s) g_\sigma g_\omega^2 \omega_0$	0

value. Noteworthy is the parametrization of IU FSU, for which the following values were obtained: $E_{\text{sym2}}^{\text{kin}}(n_0) = 17.93$ MeV, $E_{\text{sym2}}^{\text{pot}}(n_0) = 13.36$ MeV, $E_{\text{sym4}}^{\text{kin}}(n_0) = 0.76$ MeV, $E_{\text{sym4}}^{\text{pot}}(n_0) = 0.41$ MeV. The second- and fourth-order symmetry energy dependence on density is characterized by a sequence of coefficients $E_{\text{sym,2}}(n_0)$, $L_{\text{sym,2}}$, $K_{\text{sym,2}}$, $E_{\text{sym,4}}(n_0)$, $L_{\text{sym,4}}$, $K_{\text{sym,4}}$. Their values are collected in Table IV.

The additional analysis presented in this paper aims to identify the extent to which the above-mentioned coefficients impact a neutron star crust-core transition density and pressure, which profoundly affect neutron star crustal phenomena. As such, significant theoretical and observational efforts are being made to infer the details of the role of the neutron star crust in this context. The equilibrium proton fractions Y_p^{eq} for the considered groups of models are presented in Fig. 6. Many surveys attempt to measure correlations among coefficients in the Taylor expansion of the function $E_{\text{asym}}(n_b)$. Based on the reported results, some crucial predictions concerning the neutron star crust-core transition density and pressure dependence on the coefficients characterizing the symmetry energy have been formulated.

The starting point of the analysis was to check correlations between the leading coefficients of the Taylor expansion (3). The study of the correlation between $L_{\text{sym,2}}$ and $E_{\text{sym,2}}(n_0)$ shows that it is positive and strong both for individual groups of models and for the entire sample (Table V), for which the the regression function is of the form $\hat{L}_{\text{sym,2}} = -177.47 + 7.6 E_{\text{sym,2}}(n_0)$, where $\hat{L}_{\text{sym,2}}$ is the conditional mean of $L_{\text{sym,2}}$

(see Appendix 1). The regression analysis considering the fourth-order correction leads to similar conclusions. In this case, the regression function for the entire sample is given by $\hat{L}_{\text{sym,24}} = -173.19 + 7.36 E_{\text{sym,24}}$, (Table V). The subscript 24 denotes a quantity obtained as a sum of the second- and fourth-order contributions in the Taylor expansion. The regression lines that summarize the relations between $L_{\text{sym,2}}$ and $E_{\text{sym,2}}$, and $L_{\text{sym,24}}$ and $E_{\text{sym,24}}$ are given in Fig. 7.

A different result was obtained for the correlation between $K_{\text{sym,2}}$ and $L_{\text{sym,2}}$ (Table VI). Compared to the previous case, this correlation is weaker and is negative for all groups except group II. It is of moderate strength for groups I and II, although it is pretty strong for group III. But, it practically disappears for the sample covering all models. This tendency is confirmed and strengthened by the correlation between $L_{\text{sym,24}}$ and $K_{\text{sym,24}}$, i.e., the cases where fourth-order terms are included. The regression lines summarizing the relations between $K_{\text{sym,2}}$ and $L_{\text{sym,2}}$, and $K_{\text{sym,24}}$ and $L_{\text{sym,24}}$ are presented in Fig. 8.

The conducted correlation analysis between the main characteristics of the function $E_{\text{sym}}(n_b)$, namely the correlations between $L_{\text{sym,2}}$ and $E_{\text{sym,2}}(n_0)$ and between $K_{\text{sym,2}}$ and $L_{\text{sym,2}}$, indicates a significant difference between them. Expressing the correlation strength by variance inflation factor (VIF), defined as $\text{VIF}_X = \frac{1}{1-R_X^2}$, where X is the reference factor, Appendix 5, the following results are obtained.

In the case of the correlation between L_{sym} and $E_{\text{sym}}(n_0)$, L_{sym} or $E_{\text{sym}}(n_0)$ may be taken as the X factor. By the ranges

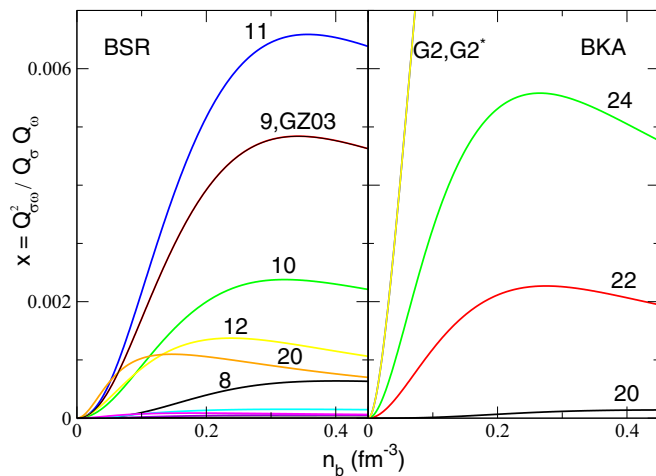
FIG. 4. The factor x as a function of density for group I (left panel) and II (right panel); it vanishes for group III.
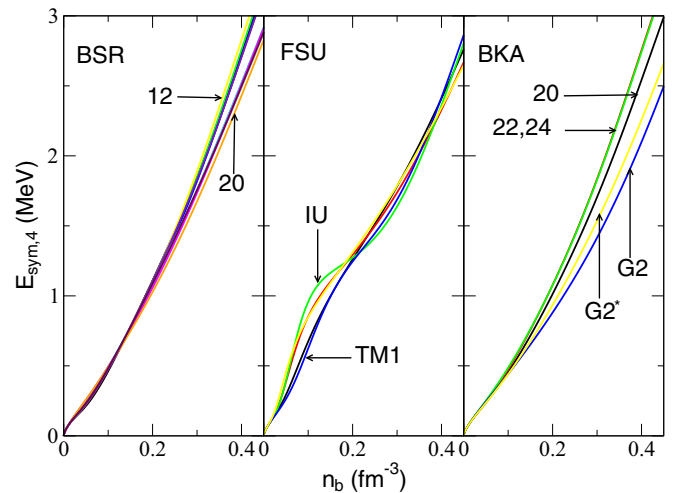

FIG. 5. The dependence on the density of the symmetry energy $E_{\text{sym,4}}$ for three distinguished groups of models.

TABLE IV. Saturation properties of the second- $[E_{\text{sym},2}(n_b)]$ and fourth-order symmetry energy $[E_{\text{sym},4}(n_b)]$: symmetry energy coefficients $E_{\text{sym},2}(n_0)$ and $E_{\text{sym},4}(n_0)$, their slopes $L_{\text{sym},2}$ and $L_{\text{sym},4}$ and curvatures $K_{\text{sym},2}$ and $K_{\text{sym},4}$.

Model	n_0 (fm^{-3})	$E_{\text{sym},2}(n_0)$ (MeV)	$L_{\text{sym},2}$ (MeV)	$K_{\text{sym},2}$ (MeV)	$E_{\text{sym},4}(n_0)$ (MeV)	$L_{\text{sym},4}$ (MeV)	$K_{\text{sym},4}$ (MeV)
BSR8	0.1469	31.07	60.24	−0.76	0.756	2.89	1.39
BSR9	0.1473	31.61	63.89	−11.33	0.762	2.80	1.63
BSR10	0.1474	32.72	70.82	−16.52	0.762	2.76	2.17
BSR11	0.1467	33.68	78.77	−24.72	0.745	2.61	2.72
BSR12	0.1473	33.99	77.89	−44.24	0.743	2.69	4.28
BSR15	0.1455	30.97	61.78	−21.36	0.747	2.64	1.12
BSR16	0.1456	31.24	62.33	−24.17	0.751	2.64	1.23
BSR17	0.1464	31.98	67.43	−31.59	0.740	2.61	2.03
BSR18	0.1459	32.73	72.64	−42.24	0.748	2.53	2.06
BSR19	0.1467	33.78	79.46	−50.12	0.742	2.48	2.30
BSR20	0.1461	34.53	88.02	−39.89	0.725	2.33	1.93
FSUGZ03	0.1473	31.54	63.98	−11.67	0.76	2.79	1.65
FSUGZ06	0.1457	31.17	62.42	−24.49	0.75	2.64	1.25
BKA20	0.1465	32.32	75.61	−14.87	0.70	2.45	2.82
BKA22	0.1477	33.25	79.02	−8.72	0.74	2.66	2.96
BKA24	0.1470	34.19	84.78	−14.95	0.75	2.58	2.96
G2	0.1535	36.39	100.66	−7.48	0.67	2.02	1.60
G2*	0.1537	30.41	69.74	−21.92	0.69	2.30	2.31
FSUGold	0.1483	32.59	60.49	−51.34	0.99	2.55	−4.83
FSUGold4	0.1474	31.40	51.75	−16.53	1.09	1.81	−3.72
XS	0.1484	31.83	54.96	−28.80	1.083	1.988	−1.39
TM1	0.1455	31.66	55.74	−71.55	0.965	2.794	−10.39
IU-FSU	0.1546	31.29	47.20	28.48	1.17	1.07	−4.81

for $R_X^2 \equiv R^2$ given in Appendix 3 and for the VIF given in Appendix 5, the correlation between L_{sym} and $E_{\text{sym}}(n_0)$ for both the parabolic and fourth-order approximations is strong for all individual groups of models and the entire sample (Table V). Even more, the correlations in groups I and II are very strong. Namely, VIF is equal respectively to 34.5 and 20.8 in the parabolic case and to 35.7 and 21.7,

FIG. 6. The equilibrium proton fraction Y_p^{eq} dependence on the density for three distinguished groups of models. The lowest equilibrium concentration of protons characterizes the third group, with the highest value of fourth-order symmetry energy potential contribution.

in the fourth-order approximation. Therefore, the VIF-based criterion (Appendix 5) says that L_{sym} and $E_{\text{sym}}(n_0)$ should not be entered simultaneously as independent variables into the regression model for the dependent variables, in groups I and II. In the whole sample, this correlation is strong (parabolic case) or moderate (the fourth-order case); see Table V.

The correlation between $K_{\text{sym},2}$ and $L_{\text{sym},2}$ (Table VI) is moderate for groups I and II and strong for group III. However, this correlation, according to the VIF criterion, is not very strong even in group III. The correlation between $K_{\text{sym},2}$ and $L_{\text{sym},2}$ is weak for the sample covering all models (Table VI). Considering the stability of estimators of structural parameters being coefficients of independent variables $K_{\text{sym},2}$ and $L_{\text{sym},2}$, these actual variables can be introduced simultaneously in the regression models of a dependent variable for the entire sample (Appendix 5).

Compared to the sample of 263 models analyzed in the paper by Dutra *et al.* [51], the number of models in the current document has been narrowed down to the group that meets the maximum number of experimental constraints. Thus, the carried-out calculations are based on the sample of models optimal in this sense. The choice of such a sample is one of the factors affecting the obtained results. In general, statistical analysis of theoretical models for which there is a justified concern that they do not describe the observational reality optimally implies that only correlations between models are reflected in the results. At the same time, authentic relationships between physical variables can be different. The reason is that, for the theoretical modeling alone, the
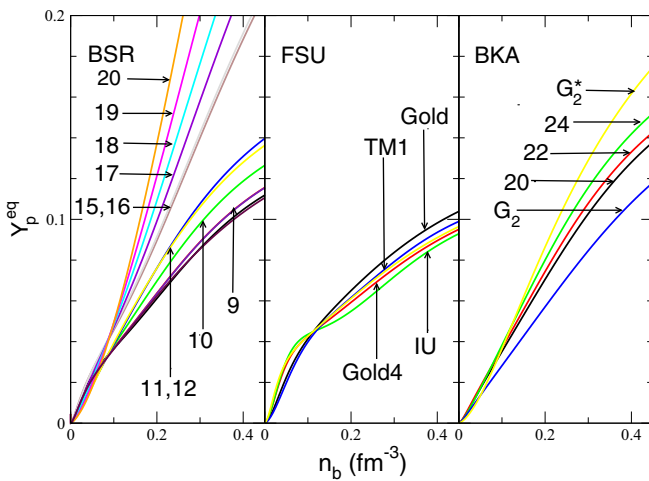
TABLE V. The characteristics of $Y \equiv L_{\mathrm{sym}}$ vs $X \equiv E_{\mathrm{sym}}$ regression for the parabolic and fourth-order approximations: the mean square due to regression MSR, the mean squared error MSE, and the coefficient of determination R^2; a and b are the estimates of the structural parameters of a particular regression model for the empirical significance level p. The sign of the Pearson linear correlation coefficient between n_t and E_{sym} agrees with the sign of b in the linear term of the regression, i.e., $r_{n_t E_{\mathrm{sym}}} = \mathrm{sgn}(b) \sqrt{R^2}$.

	a	b	MSR	MSE	R^2	p
$\hat{L}_{\mathrm{sym},2} = a + b E_{\mathrm{sym},2}$	MeV		MeV^2	MeV^2		
Group I (BSR & all)	-151.94609	6.85229	893.29848	2.45488	0.971	$<10^{-9}$
Group II (BKA, G2*, G2)	-91.04198	5.19376	529.15228	8.91087	0.952	0.005
Group III (FSUGold & all)	-225.8971	8.81521	81.72374	5.24873	0.838	0.03
All groups	-177.4703	7.59893	2648.30862	42.77592	0.747	$<10^{-6}$
$\hat{L}_{\mathrm{sym},24} = a + b E_{\mathrm{sym},24}$	MeV		MeV^2	MeV^2		
Group I (BSR & all)	-152.97528	6.80835	872.67583	2.27561	0.972	$<10^{-9}$
Group II (BKA, G2*, G2)	-90.82786	5.14986	518.2869	8.34095	0.954	0.004
Group III (FSUGold & all)	-268.90264	9.90337	83.80918	12.95099	0.683	0.08
All groups	-173.18842	7.35965	2345.49608	59.6366	0.652	$<10^{-5}$

consistency requirement necessary for data analyses must be spoken of (Appendix 2).

The analysis allows for considering the existing correlations in the context of groups of the models, which comply with the experimental constraints. If correlations are observed only for selected groups of models but are hardly visible in the entire sample, one can assume that these correlations are strongly model dependent. The obtained results indicate that compliance with the results obtained in other papers is sometimes obtained only for given groups of models. A weak correlation is obtained in the case of the correlation between K_{sym} and L_{sym} for the entire sample of models. [14,85–87]. The obtained correlations between the main symmetry energy characteristics are of great use in analyzing the properties of neutron stars. For example, in papers [88,89], the correlation results between the radius of a neutron star and symmetry energy parameters. The analysis of the relationship between

the $E_{\mathrm{sym}}(n_0)$, L_{sym}, and K_{sym} parameters and the properties of neutron stars is the subject of our current research.

B. The statistical analysis of factors determining the neutron star crust-core phase boundary.

The goal of this paper is to study relations between the main coefficients characterizing the symmetry energy and quantities relevant at the neutron star crust-core phase boundary, namely the transition density n_t, the corresponding pressure P_t, and equilibrium proton fraction $Y_p^{\mathrm{eq}}(n_t)$. The applied regression analysis allows one to study the influence of selected independent variables on the crust-core transition density n_t. The regression models were built based on the following set of independent variables: $E_{\mathrm{sym},2}$, $L_{\mathrm{sym},2}$, $K_{\mathrm{sym},2}$, K_0, $Y_{p,2}^{\mathrm{eq}}$, their squares, and $P_{t,2}$ and their counterparts in the fourth-order approximation. The presented results include only those variables for which the regression models have the highest value of R^2 (Appendix 3). The only exception has been discussed in Secs. IV B 1 and IV B 2.

1. The symmetry energy encoded in characteristics of the edge of a neutron star core

Numerous statistical analyses exist of the transition density correlation with coefficients describing the symmetry energy. The reported results are not unambiguous; therefore, a more in-depth analysis of this problem is welcome, and these issues are at the roots of this research. Constructing a hierarchy of the linear regression models will show which independent variables are suitable for describing the crust-core transition density.

Considering the coefficient of determination R^2 as a measure of the strength of a correlation for the whole sample of models, the strongest correlation occurs between factors $n_{t,2}$ and the $K_{\mathrm{sym},2}^2$ (Table VII). Additionally, also for the whole sample of models, the regression model $n_{t,2}$ against $P_{t,2}$ as the only factor does not compare well with such factors as $(Y_{p,2}^{\mathrm{eq}})^2$, $Y_{p,2}^{\mathrm{eq}}$ (Table VIII), K_0^2, and K_0 (Table IX), although it outperforms the cases with factors $K_{\mathrm{sym},2}$, $E_{\mathrm{sym},2}^2(n_0)$, $E_{\mathrm{sym},2}(n_0)$, $L_{\mathrm{sym},2}$, and $L_{\mathrm{sym},2}^2$. The existence of a strong correlation
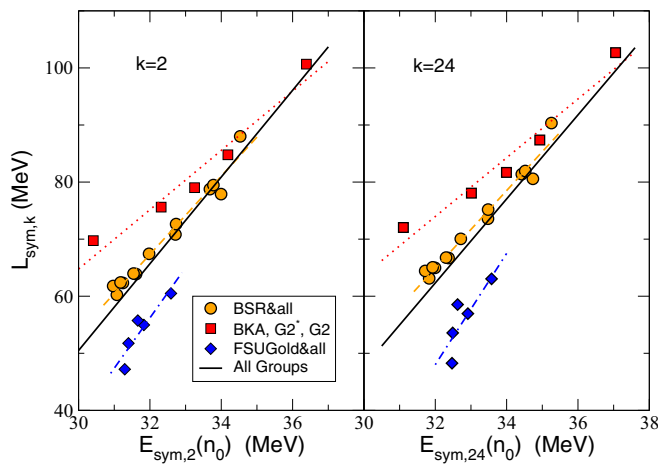

FIG. 7. The dependence L_{sym} on $E_{\mathrm{sym}}(n_0)$. In the left panel, dashed lines represent the regression lines obtained for individual groups, whereas the black straight line corresponds to the regression analysis results performed for the entire sample of models. The right panel shows analogous results after considering fourth-order terms in the Taylor expansion.

TABLE VI. The characteristics of $Y \equiv K_{\mathrm{sym}}$ vs $X \equiv L_{\mathrm{sym}}$ regression for the parabolic and fourth-order approximations: the mean square due to regression MSR, the mean squared error MSE, and the coefficient of determination R^2, where a and b are the estimates of the structural parameters of a particular regression model for the empirical significance level p. The sign of the Pearson linear correlation coefficient between K_{sym} and L_{sym} agrees with the sign of b in the linear term of the regression, i.e., $r_{K_{\mathrm{sym}}L_{\mathrm{sym}}} = \mathrm{sgn}(b)\sqrt{R^2}$.

	a	b	MSR	MSE	R^2	p
$K_{\mathrm{sym},2} = a + b\,L_{\mathrm{sym},2}$	MeV		MeV^2	MeV^2		
Group I (BSR & all)	58.6152	-1.21485	1358.24242	110.74235	0.527	0.005
Group II (BKA, G2*, G2)	-43.97695	0.37074	76.4046	19.18188	0.57	0.14
Group III (FSUGold & all)	325.84887	-6.54812	4179.30806	528.03821	0.725	0.07
All groups	-12.0558	-0.17206	104.99437	431.57163	0.011	0.63
$K_{\mathrm{sym},24} = a + b\,L_{\mathrm{sym},24}$	MeV		MeV^2	MeV^2		
Group I (BSR & all)	59.85996	-1.16044	1208.86825	110.66292	0.498	0.007
Group II (BKA, G2*, G2)	-40.49781	0.34893	66.14803	21.27145	0.509	0.18
Group III (FSUGold & all)	311.71854	-6.14732	4635.35078	559.53819	0.734	0.06
All groups	-21.61385	-0.024538	2.16624	481.00552	0.0002	0.95

between n_t and P_t in groups of models (Table X) could be the first statistical premise for building a hierarchy of regression models starting from the independent variable P_t.

Detailed studies performed in the paper [89] concerning the core-crust transition density n_t and proton fraction Y_t suggested that they are correlated with L_{sym}. Analysis has been done for different models. However, the relation between L_{sym} and the transition pressure P_t was shown to be much more model dependent. Similar conclusions have been drawn based on the analysis performed in this paper. Below, it will be shown that there are more reasons behind this choice. One of the reasons is that, due to the value of R^2, the model with factors (P_t, L_{sym}) outperforms the second-ranking two-factor regression models, that is $(K_{\mathrm{sym}}, K_{\mathrm{sym}}^2)$ (Tables VII and X), for both parabolic and fourth-order approximations.

The analysis starts with the calculation of partial correlation coefficients [90,91]. Partial correlation (Appendix 6) is directly linked to correlation: if one investigates the correlation between two given variables, other variables may influence their relationship. The accurate results can only be obtained after removing the effect of possible third variables. Such an approach is adopted in this paper. Therefore, before examining the regression n_t vs P_t, the partial correlation coefficient $r_{n_t P_t | L_{\mathrm{sym}}}$ for n_t and P_t with L_{sym} under control is calculated [90–93].

The first part of the calculations considers the representation of the function describing the symmetry energy through the parabolic approximation. To determine the coefficient $r_{n_{t,2} P_{t,2} | L_{\mathrm{sym},2}}$, three correlation coefficients are needed. The relevant ones are $r_{n_{t,2} P_{t,2}} = 0.483$, $r_{n_{t,2} L_{\mathrm{sym},2}} = -0.0348$, and $r_{P_{t,2} L_{\mathrm{sym},2}} = 0.828$. It is noticed that the moderate value $r_{n_{t,2} P_{t,2}} = 0.483$ jumps to a higher value $r_{n_{t,2} P_{t,2} | L_{\mathrm{sym},2}} = 0.9151$. This large influence of $L_{\mathrm{sym},2}$ on the correlation between $n_{t,2}$ and $P_{t,2}$ lies in the residuals of the regression model $n_{t,2}$ vs $P_{t,2}$ [90]. Therefore, the solution to the problem of better fitting to the sample points is to extend the regression model $n_{t,2}$ vs $P_{t,2}$ to the model with factors $(P_{t,2}, L_{\mathrm{sym},2})$. From the partial correlation coefficient analysis, it appears that taking $L_{\mathrm{sym},2}$ under control reveals a very strong (devoid of the influence of $L_{\mathrm{sym},2}$) direct correlation (Appendix 6) between $n_{t,2}$ and $P_{t,2}$ even in the whole sample of models. As an illustration the regression lines summarizing the relations between $n_{t,2}$ and $P_{t,2}$ and between $n_{t,24}$ and $P_{t,24}$ are presented in Fig. 9. The analysis of the other significant partial correlations will be performed later.

Type II sum of squares (SS) (Appendix 4) is another method justifying the choice of P_t as the first independent variable in constructing the hierarchy of regression models. The model with factors $(P_{t,2}, L_{\mathrm{sym},2})$ can be reduced to either $(L_{\mathrm{sym},2})$ or $(P_{t,2})$. In the first case the obtained type II SS is $\mathrm{SS}(P_{t,2} | L_{\mathrm{sym},2}) = 4.3875 \times 10^{-4}$, and in the second case $\mathrm{SS}(L_{\mathrm{sym},2} | P_{t,2}) = 3.1684 \times 10^{-4}$. This means that reducing the higher hierarchical model $(P_{t,2}, L_{\mathrm{sym},2})$ to $(P_{t,2})$ is less harmful to the goodness of the fit than reducing $(P_{t,2}, L_{\mathrm{sym},2})$ to $(L_{\mathrm{sym},2})$ alone. This suggests that when building the model $(P_{t,2}, L_{\mathrm{sym},2})$, $P_{t,2}$ should be introduced first as a factor on which $n_{t,2}$ depends. Then, eventually, this procedure can be extended by adding $L_{\mathrm{sym},2}$. However, neglecting the

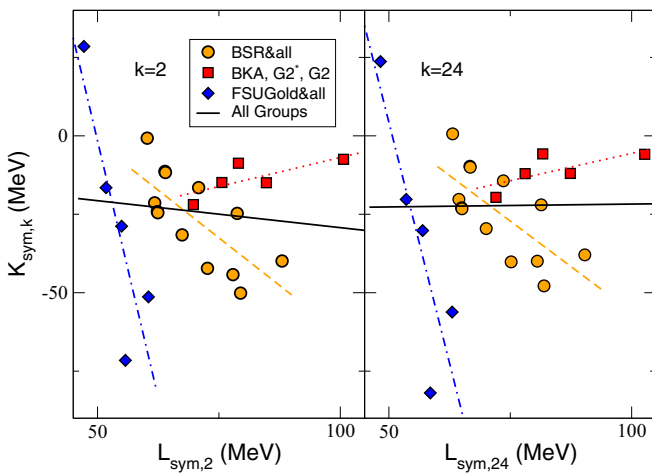FIG. 8. The dependence K_{sym} on L_{sym}. In the left panel, dashed lines represent the regression lines obtained for individual groups. The right panel shows analogous results after considering fourth-order terms in the Taylor expansion. Due to the lack of correlation when the whole sample of models is considered, the regression line, in this case, is not marked.

TABLE VII. The characteristics of $Y \equiv n_t$ vs $X \equiv K_{sym}^2$ and $Y \equiv n_t$ vs $X \equiv (K_{sym}, K_{sym}^2)$ regressions: the mean square due to regression MSR, the mean squared error MSE, and the coefficient of determination R^2, where a, b, and c are the estimates of the structural parameters of a particular regression model for the empirical significance level p. The sign of the Pearson linear correlation coefficient between n_t and K_{sym}^2 in the regression $\hat{n}_t = a + b K_{sym}^2$ agrees with the sign of b in the linear term of the regression, i.e., $r_{n_t K_{sym}^2} = \text{sgn}(b) \sqrt{R^2}$.

	a	b	c	MSR	*MSE*	R^2	p
$\hat{n}_{t,2} = a + b K_{sym,2}^2$	fm^{-3}	MeV^{-2} fm^{-3}		fm^{-6}	fm^{-6}		
Group I (BSR & all)	0.076316	2.99457×10^{-6}		7.02666×10^{-5}	3.43843×10^{-6}	0.65	0.001
Group II (BKA, G2*, G2)	0.08152	-1.36327×10^{-6}		2.14099×10^{-7}	1.53097×10^{-5}	0.005	0.91
Group III (FSUGold & all)	0.081699	2.40147×10^{-6}		9.15593×10^{-5}	2.7916×10^{-5}	0.522	0.17
All groups	0.078349	2.80879×10^{-6}		0.000247898	1.31771×10^{-5}	0.473	0.0003
$\hat{n}_{t,2} = a + b K_{sym,2} + c K_{sym,2}^2$	fm^{-3}	MeV^{-1} fm^{-3}	MeV^{-2} fm^{-3}	fm^{-6}	fm^{-6}		
All groups	0.080459	0.00020043	5.5757×10^{-6}	0.00018782	7.44851×10^{-6}	0.716	$<10^{-5}$
$\hat{n}_{t,24} = a + b K_{sym,24}^2$	fm^{-3}	MeV^{-2} fm^{-3}		fm^{-6}	fm^{-6}		
Group I (BSR & all)	0.075359	2.25268×10^{-6}		3.19356×10^{-5}	2.45133×10^{-6}	0.542	0.004
Group II (BKA, G2*, G2)	0.077856	2.70655×10^{-6}		6.01721×10^{-7}	8.17361×10^{-6}	0.024	0.8
Group III (FSUGold & all)	0.082795	1.48893×10^{-6}		6.36808×10^{-5}	3.78248×10^{-5}	0.359	0.29
All groups	0.077024	2.3736×10^{-6}		0.00027298	1.42773×10^{-5}	0.477	0.0003
$\hat{n}_{t,24} = a + b K_{sym,24} + c K_{sym,24}^2$	fm^{-3}	MeV^{-1} fm^{-3}	MeV^{-2} fm^{-3}	fm^{-6}	fm^{-6}		
All groups	0.079818	0.00024953	5.45594×10^{-6}	0.00022085	6.55494×10^{-6}	0.771	$<10^{-6}$

influence of $L_{sym,2}$ makes the impact of this factor fall into the residuals (errors) of the $n_{t,2}$ vs $P_{t,2}$ regression model. This fact has already been noticed in the analysis of the partial correlation coefficient $r_{n_{t,2}P_{t,2}|L_{sym,2}}$. Consequently, the strong correlations between $n_{t,2}$ and $P_{t,2}$ in groups I, II, and III suggest that $L_{sym,2}$ explains the group differentiation. The $L_{sym,2}$ factor is also responsible for the high dispersion of pairs $(P_{t,2}, n_{t,2})$ around the regression line $\hat{n}_{t,2} = 0.0753 + 0.0122 P_{t,2}$ for the whole sample of models (see Table X). The above conclusion is reinforced by the fact that for the whole sample of models, the values of the partial correlation coefficients $r_{n_{t,2}P_{t,2}|K_{sym,2}} = 0.425$, $r_{n_{t,2}K_{sym,2}|L_{sym,2}} = -0.27$, $r_{n_{t,2}L_{sym,2}|K_{sym,2}} = -0.066$ are much smaller than $r_{n_{t,2}P_{t,2}|L_{sym,2}} = 0.9151$. The multiple correlation coefficient $R_{n_{t,2}|P_{t,2},L_{sym,2}} = 0.9152$, describing the strength of the correlation between $n_{t,2}$ and the group of variables $(P_{t,2}, L_{sym,2})$, and the multiple correlation coefficient $R_{n_{t,2}|P_{t,2},L_{sym,2},K_{sym,2}} = 0.917$, describing the strength of the correlation between $n_{t,2}$ and the group of variables $(P_{t,2}, L_{sym,2}, K_{sym,2})$, hardly change if compared to the value of $r_{n_{t,2}P_{t,2}|L_{sym,2}}$. On the other hand, the value of $R_{n_{t,2}|P_{t,2},L_{sym,2},K_{sym,2}} = 0.917$ means that practically all the

variability of $n_{t,2}$ is explained by the group of variables $(P_{t,2}, L_{sym,2}, K_{sym,2})$. Hence the adopted maximal regression model is $n_{t,2}$ vs $(P_{t,2}, L_{sym,2}, K_{sym,2})$. The standard error values of the estimators of the parameters of the $n_{t,2}$ vs $(P_{t,2})$, $(P_{t,2}, L_{sym,2})$ and $(P_{t,2}, L_{sym,2}, K_{sym,2})$ regression models are collected in Table XI. The residuals for regression models $n_{t,2}$ vs $(P_{t,2}, L_{sym,2})$ and $(P_{t,2}, L_{sym,2}, K_{sym,2})$ pass the Kolmogorov-Smirnov test for normality at the significance levels of 0.01 and 0.15, respectively.

Remodeling the symmetry energy by including the fourth-order term in the Taylor expansion (3) modifies the obtained results. According to the decreasing values of R^2 and for the whole sample of models, there is the following order of factors correlated with $n_{t,24}$: $(Y_{p,24}^{eq})^2$, $K_{sym,24}^2$, $Y_{p,24}^{eq}$, K_0^2, $P_{t,24}$ (see Tables VIII and IX), $K_{sym,24}$, $L_{sym,24}$, $L_{sym,24}^2$ $E_{sym,24}$, $E_{sym,24}^2$. For the entire sample, the correlation strength between $n_{t,24}$ and both $Y_{p,24}^{eq}$ and $(Y_{p,24}^{eq})^2$ increases when the fourth-order approximation is included (Table VIII).

The model with factors $(P_{t,24}, L_{sym,24})$ also outperforms the second-ranking two-factor regression models, that is $(K_{sym,24}, K_{sym,24}^2)$ (Tables VII and X). The model with

TABLE VIII. The characteristics of $Y \equiv n_t$ vs $X \equiv Y_p$ and $X \equiv Y_p^2$ regressions: the mean square due to regression MSR, the mean squared error MSE, and the coefficient of determination R^2, where a and b are the estimates of the structural parameters of a particular regression model for the empirical significance level p. The Pearson correlation coefficient between n_t and Y_p is $r_{n_t Y_p} = \text{sgn}(b) \sqrt{R^2}$.

	a	b	MSR	MSE	R^2	p
$\hat{n}_{t,2} = a + b Y_{p,2}$	fm^{-3}	fm^{-3}	fm^{-6}	fm^{-6}		
All groups	0.058583	0.77317	0.00015885	1.74175×10^{-5}	0.303	0.01
$\hat{n}_{t,2} = a + b Y_{p,2}^2$						
All groups	0.069344	13.67456	0.00017781	1.65148×10^{-5}	0.339	0.004
$\hat{n}_{t,24} = a + b Y_{p,24}$						
All groups	0.056255	0.7424	0.00026212	0.00026212	0.458	0.0004
$\hat{n}_{t,24} = a + b Y_{p,24}^2$						
All groups	0.067872	11.61228	0.00028384	1.37603×10^{-5}	0.496	0.0002

TABLE IX. The characteristics of $Y \equiv n_{t,2}$ (and $Y \equiv n_{t,24}$) vs $X \equiv K_0^2$ or K_0 regressions: the mean square due to regression MSR, the mean squared error MSE, and the coefficient of determination R^2 (Appendix 3). a and b are the estimates of the structural parameters of a particular regression model for the empirical significance level p. The sign of the Pearson linear correlation coefficient between $Y \equiv n_{t,2}$ ($Y \equiv n_{t,24}$) and $X \equiv K_0^2$ or K_0 agrees with the sign of b in the linear term of the regression, i.e., $r_{YX} = \mathrm{sgn}(b)\sqrt{R^2}$.

	a	b	MSR	MSE	R^2	p
$\hat{n}_{t,2} = a + b\,K_0^2$	fm^{-3}	MeV^{-1} fm^{-3}	fm^{-6}	fm^{-6}		
All groups	0.059705	4.05699×10^{-7}	0.00014627	1.80166×10^{-5}	0.279	0.01
$\hat{n}_{t,2} = a + b\,K_0$	fm^{-3}	MeV^{-1} fm^{-3}	fm^{-6}	fm^{-6}		
All groups	0.036273	0.0001955	0.0001374	1.84388×10^{-5}	0.262	0.01
$\hat{n}_{t,24} = a + b\,K_0^2$	fm^{-3}	MeV^{-1} fm^{-3}	fm^{-6}	fm^{-6}		
All groups	0.054131	4.78932×10^{-7}	0.00020384	1.75696×10^{-5}	0.356	0.003
$\hat{n}_{t,24} = a + b\,K_0$	fm^{-3}	MeV^{-1} fm^{-3}	fm^{-6}	fm^{-6}		
All groups	0.025712	0.00023409	0.000197	1.78952×10^{-5}	0.344	0.003

factors $(P_{t,24}, L_{\mathrm{sym},24})$ can be reduced to either $(L_{\mathrm{sym},24})$ or $(P_{t,24})$. In the first case the obtained type II SS is $\mathrm{SS}(P_{t,24}|L_{\mathrm{sym},24}) = 4.3646 \times 10^{-4}$, and in the second case $\mathrm{SS}(L_{\mathrm{sym},24}|P_{t,24}) = 4.147 \times 10^{-4}$. This means that reducing the higher hierarchical model $(P_{t,24}, L_{\mathrm{sym},24})$ to $(P_{t,24})$ is still less harmful to the goodness of the fit than reducing it to $(L_{\mathrm{sym},24})$ alone, although the difference is smaller than in the parabolic case. Thus, building a regression model $n_{t,24}$

TABLE X. The characteristics of the regression of $Y \equiv n_{t,2}$ vs $X \equiv P_{t,2}$ or $X \equiv (P_{t,2}, L_{\mathrm{sym},2})$ or $X \equiv (P_{t,2}, L_{\mathrm{sym},2}, K_{\mathrm{sym},2})$: the mean square due to regression MSR, the mean squared error MSE, and the coefficient of determination R^2, where a, b, c, and d are the estimates of the structural parameters of a particular regression model for the empirical significance level p. The Pearson correlation coefficient between n_t and P_t in the regression $\hat{n}_t = a + b\,P_t$ is $r_{n_t P_t} = \mathrm{sgn}(b)\sqrt{R^2}$.

|	a	b	c	d	MSR	MSE	R^2	p
$\hat{n}_{t,2} = a + b\,P_{t,2}$	fm^{-3}	MeV^{-1}	MeV^{-1} fm^{-3}	MeV^{-1} fm^{-3}	fm^{-6}	fm^{-6}		
Group I (BSR & all)	0.071632	0.015961			9.82314×10^{-5}	8.96171×10^{-7}	0.909	$<10^{-6}$
Group II (BKA, G2*, G2)	0.072688	0.014211			2.94546×10^{-5}	5.56289×10^{-6}	0.638	0.1
Group III (FSUGold & all)	0.077041	0.024651			9.60264×10^{-5}	2.64269×10^{-5}	0.548	0.15
All groups	0.075288	0.012231			0.00012255	1.91462×10^{-5}	0.234	0.02
$\hat{n}_{t,2} = a + b\,P_{t,2} + c\,L_{\mathrm{sym},2}$								
Group I (BSR & all)	0.0896	0.033668	-0.00037351		5.28702×10^{-5}	2.34877×10^{-7}	0.978	$<10^{-8}$
Group II (BKA, G2*, G2)	0.10431	0.055473	-0.00068843		2.22889×10^{-5}	7.82724×10^{-7}	0.966	0.03
Group III (FSUGold & all)	0.12885	0.04028	-0.001068		8.43015×10^{-5}	3.35212×10^{-6}	0.962	0.04
All groups	0.098399	0.041324	-0.0005337		0.00021969	4.26152×10^{-6}	0.838	$<10^{-7}$
$\hat{n}_{t,2} = a + b\,P_{t,2} + c\,L_{\mathrm{sym},2}$ $+ d\,K_{\mathrm{sym},2}$								
Group I (BSR & all)	0.092081	0.039342	-0.00042845	4.75418×10^{-5}	3.59226×10^{-5}	3.5726×10^{-8}	0.997	$<10^{-10}$
Group II (BKA, G2*, G2)	0.12409	0.07011	-0.0010005	0.00022088	1.51972×10^{-5}	5.51623×10^{-7}	0.988	0.14
Group III (FSUGold & all)	0.11265	0.045096	-0.00076925	6.3074×10^{-5}	5.75042×10^{-5}	2.79473×10^{-6}	0.984	0.16
All groups	0.10408	0.052582	-0.00065805	0.00010105	0.00016646	1.32869×10^{-6}	0.952	$<10^{-11}$
$\hat{n}_{t,24} = a + b\,P_{t,24}$								
Group I (BSR & all)	0.071324	0.013069			4.76008×10^{-5}	1.02723×10^{-6}	0.808	$<10^{-4}$
Group II (BKA, G2*, G2)	0.072381	0.010676			1.00983×10^{-5}	5.00809×10^{-6}	0.402	0.25
Group III (FSUGold & all)	0.076335	0.024156			8.70972×10^{-5}	3.00194×10^{-5}	0.492	0.19
All groups	0.074125	0.011386			7.4197×10^{-5}	2.37432×10^{-5}	0.13	0.09
$\hat{n}_{t,24} = a + b\,P_{t,24} + c\,L_{\mathrm{sym},24}$								
Group I (BSR & all)	0.08905	0.033155	-0.00036682		2.79707×10^{-5}	2.95889×10^{-7}	0.95	$<10^{-6}$
Group II (BKA, G2*, G2)	0.10068	0.061474	-0.00066683		1.15222×10^{-5}	1.03903×10^{-6}	0.917	0.08
Group III (FSUGold & all)	0.12605	0.040517	-0.001007		8.57682×10^{-5}	2.80944×10^{-6}	0.968	0.03
All groups	0.096677	0.041234	-0.00050694		0.00024445	4.19542×10^{-6}	0.854	$<10^{-8}$
$\hat{n}_{t,24} = a + b\,P_{t,24}$ $+ c\,L_{\mathrm{sym},24} + d\,K_{\mathrm{sym},24}$								
Group I (BSR & all)	0.090736	0.038966	-0.00040919	4.86088×10^{-5}	1.93893×10^{-5}	8.13773×10^{-8}	0.988	$<10^{-8}$
Group II (BKA, G2*, G2)	0.13212	0.096521	-0.0012229	0.00034574	8.28011×10^{-6}	2.82223×10^{-7}	0.989	0.13
Group III (FSUGold & all)	0.11244	0.044959	-0.0007654	5.35919×10^{-5}	5.81194×10^{-5}	2.79715×10^{-6}	0.984	0.16
All groups	0.10141	0.053666	-0.00062099	9.80938×10^{-5}	0.00018214	1.38883×10^{-6}	0.954	$<10^{-12}$
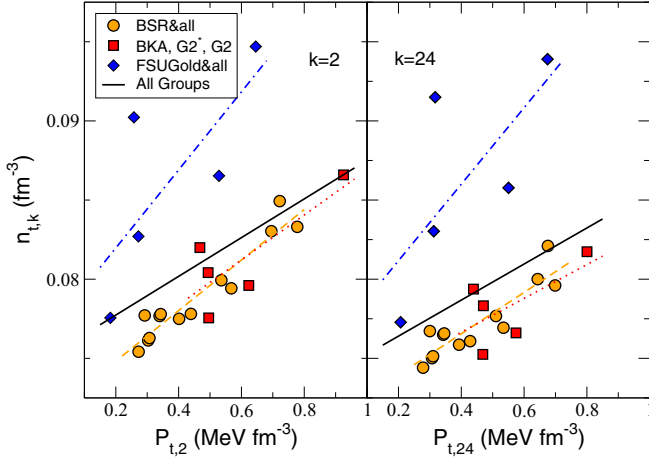
FIG. 9. The dependence of the transition density n_t on the corresponding transition pressure P_t. In the left panel, dashed lines represent the regression lines obtained for individual groups. The right panel shows analogous results with fourth-order terms in the Taylor expansion.

vs $(P_{t,24}, L_{\text{sym},24})$, one should introduce $P_{t,24}$ first as a factor. Values of three correlation coefficients are necessary to determine the value of $r_{n_{t,24}P_{t,24}|L_{24}}$ (Appendix 6). The relevant ones are $r_{n_{t,24}P_{t,24}} = 0.36$, $r_{n_{t,24}L_{\text{sym},24}} = -0.303$, and $r_{P_{t,24}L_{\text{sym},24}} = 0.743$. Their values have changed if compared to their parabolic approximation counterparts. The discussed partial correlation coefficient for the whole sample of models is $r_{n_{t,24}P_{t,24}|L_{24}} = 0.916$. Its value is almost the same as in the parabolic case. The other coefficients $r_{n_{t,24}P_{t,24}|K_{24}} = 0.262$, $r_{n_{t,24}K_{24}|L_{24}} = -0.329$, $r_{n_{t,24}L_{24}|K_{24}} = -0.323$ are much smaller than $r_{n_{t,24}P_{t,24}|L_{24}}$. They also differ from their parabolic approximation counterparts. The multiple correlation coefficients $R_{n_{t,24}|P_{t,24},L_{24}} = 0.924$ and $R_{n_{t,24}|P_{t,24},L_{24},K_{24}} = 0.977$ are higher than their parabolic approximation counterparts. Comparing the increase of $r_{n_{t,24}P_{t,24}|L_{24}}$ to the value of $R_{n_{t,24}|P_{t,24},L_{24}}$ and then to $R_{n_{t,24}|P_{t,24},L_{24},K_{24}}$, it is seen that the effect of $L_{\text{sym},24}$ after $P_{t,24}$, and especially the effect of $K_{sym,24}$ added after $L_{\text{sym},24}$ to explain $n_{t,24}$, are more significant than in the parabolic case. The correlation between $n_{t,24}$ and $P_{t,24}$ in group I is strong, but in groups II and III it is moderate. Comparing the values $r_{n_{t,24}P_{t,24}} = 0.36$ and $r_{n_{t,24}P_{t,24}|L_{\text{sym},24}} = 0.916$ for the whole sample of models, the same conclusion as in the case of the parabolic approximation can be drawn; namely, the $L_{\text{sym},24}$ factor is still responsible for group differentiation and for the high dispersion of pairs $(P_{t,24}, n_{t,24})$ around the regression line $\hat{n}_{t,24} = 0.0741 + 0.0114 P_{t,24}$ for the whole sample of models (Table X). The value $R_{n_{t,24}|P_{t,24},L_{\text{sym},24},K_{\text{sym},24}} = 0.977$ suggests that practically all the variability of $n_{t,24}$ is explained by a group of variables $(P_{t,24}, L_{\text{sym},24}, K_{\text{sym},24})$. Hence the adopted maximal model is $(P_{t,24}, L_{\text{sym},24}, K_{\text{sym},24})$. Finally, the standard error values of the estimators of the parameters of the $n_{t,24}$ vs $(P_{t,24})$, $(P_{t,24}, L_{\text{sym},24})$, and $(P_{t,24}, L_{\text{sym},24}, K_{\text{sym},24})$ regression models are given in Table XI. The residuals for regression models $n_{t,24}$ vs $(P_{t,24}, L_{\text{sym},24})$ and $(P_{t,24}, L_{\text{sym},24}, K_{\text{sym},24})$ pass the Kolmogorov-Smirnov test for normality at the significance levels of 0.05 and 0.1, respectively.

2. The analysis of the n_t versus P_t, L_{sym}, K_{sym} regression via types I and II SS

The results of using type I sum of squares (SS) in a hierarchical building of the regression model for n_t vs chosen factors in the parabolic and fourth-order approximations are presented in Table XIII. Due to the higher value of R^2 in the model with factors (P_t, L_{sym}) than in the second-ranking two-factor regression model $(K_{\text{sym}}, K_{\text{sym}}^2)$ (Tables VII and X), the construction of the hierarchy of regression models starts with the model with P_t only. The legitimacy of such an approach

TABLE XI. The regression functions $\hat{n}_t = a + b P_t$, $\hat{n}_t = a + b P_t + c L_{\text{sym}}$, and $\hat{n}_t = a + b P_t + c L_{\text{sym}} + d K_{\text{sym}}$ give the approximations of the expectation values $n_t^{\text{th}} = \alpha_0 + \alpha_1 P_t$, $n_t^{\text{th}} = \alpha_0 + \alpha_1 P_t + \alpha_2 L_{\text{sym}}$, and $n_t^{\text{th}} = \alpha_0 + \alpha_1 P_t + \alpha_2 L_{\text{sym}} + \alpha_3 K_{\text{sym}}$, respectively. The estimates a, b, c, and d are the values of the estimators $\hat{\alpha}_i$, $i = 0, 1, 2, 3$, of the structural parameters α_i, $i = 0, 1, 2, 3$, and $\hat{\sigma}_{\hat{\alpha}_i}$, $i = 0, 1, 2, 3$, are the corresponding standard errors of $\hat{\alpha}_i$.

	$\hat{\alpha}_0 = a$	$\hat{\alpha}_1 = b$	$\hat{\alpha}_2 = c$	$\hat{\alpha}_3 = d$	$\hat{\sigma}_{\hat{\alpha}_0}$	$\hat{\sigma}_{\hat{\alpha}_1}$	$\hat{\sigma}_{\hat{\alpha}_2}$	$\hat{\sigma}_{\hat{\alpha}_3}$
	fm^{-3}	MeV^{-1}	MeV^{-1} fm^{-3}	MeV^{-1} fm^{-3}	fm^{-3}	MeV^{-1}	MeV^{-1} fm^{-3}	MeV^{-1} fm^{-3}
$\hat{n}_{t,2} = a + b P_{t,2}$								
All groups	0.075288	0.012231			0.0024642	0.0048346		
$\hat{n}_{t,2} = a + b P_{t,2} + c L_{\text{sym},2}$								
All groups	0.098399	0.041324	-0.0005337		0.0029216	0.0040727	6.18949×10^{-5}	
$\hat{n}_{t,2} = a + b P_{t,2}$ $+ c L_{\text{sym},2} + d K_{\text{sym},2}$								
All groups	0.10408	0.052582	-0.00065805	0.00010105	0.0018376	0.0028246	3.92041×10^{-5}	1.50393×10^{-5}
$\hat{n}_{t,24} = a + b P_{t,24}$								
All groups	0.074125	0.011386			0.0031326	0.0064408		
$\hat{n}_{t,24} = a + b P_{t,24}$ $+ c L_{\text{sym},24}$								
All groups	0.096677	0.041234	-0.00050694		0.0026229	0.0040427	5.09896×10^{-5}	
$\hat{n}_{t,24} = a + b P_{t,24}$ $+ c L_{\text{sym},24} + d K_{\text{sym},24}$								
All groups	0.10141	0.053666	-0.00062099	9.80938×10^{-5}	0.0016789	0.0030236	3.42737×10^{-5}	1.52425×10^{-5}

TABLE XII. The characteristics of n_t vs $L_{\rm sym}$, n_t vs $K_{\rm sym}$, n_t vs $(L_{\rm sym}, K_{\rm sym})$ and $L_{\rm sym,2}$ vs $P_{t,2}$ regressions in the whole sample for the parabolic and fourth-order approximations: the mean square due to regression MSR, the mean squared error MSE, and the coefficient of determination R^2. a, b, and c are the estimates of the structural parameters of a particular regression model for the empirical significance level p. For the regression $K_{\rm sym}$ vs $L_{\rm sym}$ see Table VI. The sign of the Pearson linear correlation coefficient between variables Y and X agrees with the sign of b in the regression function of the type $\hat{Y} = a + bX$, i.e., $r_{YX}^2 = {\rm sgn}(b)\sqrt{R^2}$.

	a	b		MSR	MSE	R^2	p
$\hat{n}_{t,2} = a + b L_{\rm sym,2}$	fm^{-3}	MeV^{-1} fm^{-3}		fm^{-6}	fm^{-6}		
All groups	0.082005	-1.33923×10^{-5}		6.36096×10^{-7}	2.49515×10^{-5}	0.001	0.87
$\hat{n}_{t,24} = a + b L_{\rm sym,24}$							
All groups	0.088004	-0.00012072		5.24345×10^{-5}	2.47795×10^{-5}	0.092	0.16
	a	b		MSR	MSE	R^2	p
$\hat{n}_{t,2} = a + b K_{\rm sym,2}$	fm^{-3}	MeV^{-1} fm^{-3}		fm^{-6}	fm^{-6}		
All groups	0.079561	-6.33728×10^{-5}		3.68197×10^{-5}	2.32285×10^{-5}	0.07	0.22
$\hat{n}_{t,24} = a + b K_{\rm sym,24}$							
All groups	0.077641	-7.3687×10^{-5}		5.48586×10^{-5}	2.46641×10^{-5}	0.096	0.15
	a	b	c	MSR	MSE	R^2	p
$\hat{n}_{t,2} = a + b L_{\rm sym,2} + c K_{\rm sym,2}$	fm^{-3}	MeV^{-1} fm^{-3}	MeV^{-1} fm^{-3}	fm^{-6}	fm^{-6}		
All groups	0.081221	-0.00002458	-0.00006501	1.94687×10^{-5}	2.4284×10^{-5}	0.074	0.46
$\hat{n}_{t,24} = a + b L_{\rm sym,24} + c K_{\rm sym,24}$							
All groups	0.086388	-0.00012256	-7.47579×10^{-5}	5.44435×10^{-5}	2.31958×10^{-5}	0.19	0.12
	a	b		MSR	MSE	R^2	p
$\hat{L}_{\rm sym,2} = a + b P_{t,2}$	MeV	fm^3		MeV^2	MeV^2		
All groups	43.30356	54.51278		2434.22106	52.97057	0.686	$<10^{-5}$
$\hat{L}_{\rm sym,24} = a + b P_{t,24}$	MeV	fm^3		MeV^2	MeV^2		
All groups	44.48693	58.879		1984.20258	76.84106	0.551	$<10^{-4}$

is supported by the analysis presented in Sec. IV B 1. From Table XIII, it is seen that the group of factors in the selected hierarchy are $(P_{t,2})$, $(P_{t,2}, L_{\rm sym,2})$ and $(P_{t,2}, L_{\rm sym,2}, K_{\rm sym,2})$, where the last one is chosen to be the maximal one. A similar analysis for the fourth-order approximation leads to a hierarchy of regression models $n_{t,24}$ vs, consecutively, $(P_{t,24})$, $(P_{t,24}, L_{\rm sym,24})$ and $(P_{t,24}, L_{\rm sym,24}, K_{\rm sym,24})$; cf. Table XIII.

Then type II SS, for both the parabolic and fourth-order approximations, was used to analyze the size of the fit loss when reducing the maximum model by one of the considered factors. The obtained results are gathered in Table XIII.

In the fourth-order approximation, removing $L_{\rm sym}$ from the maximal model worsens the fit quality of the regression function if compared to removing P_t. In the parabolic approximation, the roles of $L_{\rm sym}$ and P_t are reversed in analogous regression analysis.

In the fourth-order approximation, removing $L_{\rm sym}$ from the maximal model worsens the fit quality of the regression function compared to neglecting P_t. In the parabolic approximation, it is the other way around. However, removing the factor $K_{\rm sym}$ from the maximal model to reduce the model to a simpler one brings the smallest loss of fit in both approximations, leading to the regression model n_t vs $(P_t, L_{\rm sym})$. Thus, the hierarchy of models in both the parabolic and fourth-order approximations is the same, i.e., (P_t), $(P_t, L_{\rm sym})$, and $(P_t, L_{\rm sym}, K_{\rm sym})$. The structural parameters (Appendix 1) of these regression models are given in Table X.

C. Correlations between the core-crust transition density and the slope and curvature of the symmetry energy

Based on the correlation analysis between the symmetry energy slope $L_{\rm sym}$ and curvature coefficients $K_{\rm sym}$, it becomes possible to quantify how these symmetry energy characteristics affect the crust-core transition density n_t and to estimate the individual role of each factor. This was done by checking the strength of the following correlation coefficients: $r_{n_t L_{\rm sym}}$, $r_{n_t K_{\rm sym}}$, $r_{n_t L_{\rm sym}|K_{\rm sym}}$, $r_{n_t K_{\rm sym}|L_{\rm sym}}$. Earlier calculations showed that the correlation between $K_{\rm sym,2}$ and $L_{\rm sym,2}$ is weak, $r_{K_{\rm sym,2} L_{\rm sym,2}} = -0.107$ (see Table VI, Sec. IV A). So, both variables can be used simultaneously in the regression of n_t vs $(K_{\rm sym,2}, L_{\rm sym,2})$. A similar result was obtained when considering the fourth-order term in the definition of symmetry energy; in that case, the correlation is even weaker, and $r_{K_{\rm sym,24} L_{\rm sym,24}} = -0.015$. It was found that, when the parabolic approximation represents the symmetry energy, the transition density $n_{t,2}$ is rather weakly anticorrelated with $K_{\rm sym,2}$ with the correlation coefficient equal to $r_{n_{t2} K_{\rm sym,2}} = -0.265$ (see Table XII). The correlation between $n_{t,2}$ and $L_{\rm sym,2}$ is also negative, but very weak: $r_{n_{t2} L_{\rm sym,2}} = -0.035$ (Table XII). The next step of the analysis was using the concept of partial correlation. The partial correlation of the transition density n_{t2} and $K_{\rm sym,2}$ with the slope $L_{\rm sym,2}$ under control is $r_{n_{t2} K_{\rm sym,2}|L_{\rm sym,2}} = -0.27$. Taking under control the symmetry energy curvature $K_{\rm sym,2}$, the partial correlation gives $r_{n_{t2} L_{\rm sym,2}|K_{\rm sym,2}} = -0.066$. In the case when the fourth-order term is included, the

obtained values of the correlations are $r_{n_{t24}L_{\text{sym},24}} = -0.30256$ and $r_{n_{t24}K_{\text{sym},24}} = -0.30947$ (Table XII) and those of the partial correlation coefficients are $r_{n_{t24}K_{\text{sym},24}|L_{\text{sym},24}} = -0.329$ and $r_{n_{t24}L_{\text{sym},24}|K_{\text{sym},24}} = -0.323$. The performed calculations indicate a significant role of the approximation used in determining the symmetry energy. Suppose only the parabolic approximation was taken into account. In that case, the above values of the correlation and partial correlation coefficients show that the factor correlated with n_{t2} is $K_{\text{sym},2}$, while the correlation between n_t and $L_{\text{sym},2}$ is practically negligible. Taking the sum of the second and fourth-order terms as a function representing the symmetry energy changes this result. In this case, the correlation analysis shows that both $K_{\text{sym},24}$ and $L_{\text{sym},24}$ factors are more strongly anticorrelated with $n_{t,24}$, and in the case of $L_{\text{sym},24}$ this correlation increased meaningfully. The regression line equations in the parabolic approximation have the forms $\hat{n}_{t,2} = 0.082 - 1.339 \times 10^{-5} L_{\text{sym},2}$ and $\hat{n}_{t,2} = 0.0796 - 6.337 \times 10^{-5} K_{\text{sym},2}$. In the case when both factors $L_{\text{sym},2}$ and $K_{\text{sym},2}$ are considered, $\hat{n}_{t,2} = 0.0812 - 0.0000246 L_{\text{sym},2} - 0.000065 K_{\text{sym},2}$. Taking into account the quartic-term contributions, the following results were obtained: $\hat{n}_{t,24} = 0.088 - 0.000121 L_{\text{sym},24}$ and $\hat{n}_{t,24} = 0.0776 - 7.369 \times 10^{-5} K_{\text{sym},24}$. In the case when both factors $L_{\text{sym},24}$ and $K_{\text{sym},24}$ are considered, $\hat{n}_{t,24} = 0.0864 - 0.000123 L_{\text{sym},24} - 7.476 \times 10^{-5} K_{\text{sym},24}$. The statistical significance of the regression model built with the inclusion of the fourth-order term is higher than for the parabolic approximation. This can be seen by comparing the values of the slopes of the respective regression functions and the p values in Table VI).

V. CONCLUSIONS

This paper aims to deepen the understanding of the mutual relations between the characteristics of the nuclear matter EoS and selected neutron star properties related to its core edge location [94]. With this in mind, the study of the underlying problem stated in this paper was conducted in two directions. First, the accuracy of the symmetry energy approximation was checked. To do this, it was shown that there is a need to include a term beyond the parabolic approximation to describe a function representing the symmetry energy.

The analysis of the dependence of the symmetry energy on the density in terms of the applied approximations was performed based on the RMF models, which are characterized by a sophisticated meson sector. The parametrizations allowed dividing all models into groups with a similar form of the nonlinear meson coupling terms. The obtained analytical formulas for the second- and fourth-order symmetry energy enable their in-depth analysis. Considering the symmetry energy kinetic and potential parts separately, it can be observed that in the case of the fourth-order approximation, the potential part is a small percentage of the kinetic part for most models. The exceptions are the third group of models, for which the kinetic and potential parts are of comparable value. In this case, the fourth-order symmetry energy appears to be similar to the second-order symmetry energy, for which the value of the kinetic part is comparable to the value of the potential part. The inclusion of the fourth-order term in

the description of the symmetry energy affects the characteristics of the crust-core phase boundary by changing the transition density n_t, the corresponding pressure P_t, and the value of the equilibrium proton fraction $Y_p^{\text{eq}}(n_t)$. However, the most significant impact of the fourth-order approximation was found in the correlation analysis between the transition density n_t and the leading symmetry energy characteristics, i.e., the slope L_{sym} and the curvature K_{sym}. In the case of the parabolic approximation, n_t is anticorrelated with K_{sym}, while the anticorrelation with L_{sym} is practically nonexistent. This picture changes when the fourth-order term is considered; then, it turns out that both variables K_{sym} and L_{sym} are equally anticorrelated with n_t. Thus, it can be concluded and emphasized that only, in this case, the individual role of L_{sym} in the analysis of the variability of the transition density n_t increases.

It is interesting to compare the obtained results with those reported in the paper [95], where the effect of the nonlinear ω-ρ and σ-ρ coupling terms on the crust-core transition density and pressure is studied. The dynamical spinodals are calculated to estimate the crust-core transition density and pressure for all the models. In the paper [95], several groups of relativistic mean field models are considered, which differ by mixed ω-ρ or σ-ρ meson interaction terms that were introduced to modify the density dependence of the symmetry energy.

Analyzing how the crust-core transition density n_t and pressure P_t depend on the symmetry energy slope L_{sym} of the given model, one can point out similarities between the results obtained in [95] and those in this paper. The first concerns the anticorrelation between n_t and L_{sym} presented in [95] for mixed ω-ρ and σ-ρ terms. It has been shown that the weak anticorrelation between n_t and L_{sym} exists for the entire sample of models considered in this paper. Similarly, as in [95] for models that include σ-ρ coupling terms—this concerns group I, especially BSR models—the transition pressure P_t increases with the symmetry energy slope L_{sym}. This very group of models is characterized by the symmetry energy slope $L_{\text{sym}} > 60$ MeV.

Research shows that different physical conditions, which include the presence of a magnetic field that is susceptible to the behavior of the symmetry energy, influence the neutron star's inner crust matter. Analysis carried out within a dynamic spinodal approach suggests that a magnetic field could cause extension of the nonhomogenous region with the crust-core transition shifted to higher densities [96]. This entails changes in other parameters characterizing the shell-nucleus transition, such as proton concentration and pressure. Also, the multiple correlation coefficient of n_t and the set of factors $(P_t, L_{\text{sym}}, K_{\text{sym}})$ is higher than in the parabolic approximation. The overall conclusion is that the influence of the pair of variables $(L_{\text{sym}}, K_{\text{sym}})$ on the n_t change is more meaningful than in the parabolic case.

The main goal of the statistical analysis was to find a regression model for n_t against selected factors that would fit well the optimal sample of models. This was done by building the hierarchy of regression models n_t vs (P_t), (P_t, L_{sym}), $(P_t, L_{\text{sym}}, K_{\text{sym}})$, where the last one is the maximal one, and the partial correlations and type I and II SS analyses were

used. The regression with factors $(P_t, L_{\text{sym}}, K_{\text{sym}})$, for which $R^2 = 0.952$ and 0.954 for the parabolic and fourth-order approximations, respectively, gives a good fit in the discussed optimal sample of models. Although K_{sym} is statistically significant in the maximal model $(P_t, L_{\text{sym}}, K_{\text{sym}})$, the analysis indicates that the simpler, lower model (P_t, L_{sym}) remains still preferable to other two-dimensional models. The n_t vs (P_t, L_{sym}) regression model may also be suitable for astrophysical research. Moreover, for factors P_t and L_{sym}, the VIF values are equal to 3.2 and 2.2 for the parabolic and fourth-order approximations, respectively. Therefore, from the point of view of the stability of the estimators of the structural parameters of the regression model, there is no indication to remove any of them from the n_t vs (P_t, L_{sym}) regression model. This means that the estimated regression models, $\hat{n}_{t,2} = 0.0984 + 0.0413\,P_{t,2} - 0.000534\,L_{\text{sym},2}$ for the parabolic approximation and $\hat{n}_{t,24} = 0.0967 + 0.0412\,P_{t,24} - 0.000507\,L_{\text{sym},24}$ for the fourth-order approximation, can be reliably used in another optimal sample of models. Partial correlation analysis also indicates that L_{sym} clearly explains the differentiation between groups I, II, and III. More details on the statistical methods used are given in the Appendix.

APPENDIX: THE REGRESSION ANALYSIS OF THE DISCUSSED MODELS

1. The regression function

Regression analysis aims to estimate relationships between a dependent random variable Y and one or more independent variables $X_1, X_2, \ldots, X_k$. It assesses the extent and direction of the relationship between variables. It can also determine the importance of independent variables in predicting the dependent ones. For a given model, the dependent variable Y (the response) is written as

$$Y = Y^{\text{th}} + E, \tag{A1}$$

where the superscript "th" means the theoretical value and E denotes the error, which is a random variable. In the case of a multiple linear regression model in the examined population of models, the theoretical value Y^{th} is the conditional expectation value $\mu_{Y|X_1, X_2, \ldots, X_k} \equiv \mathrm{E}[Y|X_1, X_2, \ldots, X_k]$ of Y given as follows:

$$Y^{\text{th}} = \alpha_0 + \alpha_1 X_1 + \alpha_2 X_2 + \cdots + \alpha_k X_k, \tag{A2}$$

where α_i, $i = 0, 1, 2, \ldots, k$ are the structural parameters with the intercept α_0, and X_i denote independent (explanatory) variables, also called factors.

If a sample of N models is randomly chosen from the population of models, then the corresponding regression model (A1) is estimated by

$$Y = \widehat{Y} + \widehat{E}. \tag{A3}$$

Here $\widehat{Y}$, which gives the approximation of Yth,

$$\widehat{Y} = \hat{\alpha}_0 + \hat{\alpha}_1 X_1 + \hat{\alpha}_2 X_2 + \cdots + \hat{\alpha}_k X_k, \tag{A4}$$

is the conditional mean $\widehat{\mu}_{Y|X_1, X_2, \ldots, X_k}$, that is the estimator of $\mu_{Y|X_1, X_2, \ldots, X_k}$, and $\hat{\alpha}_0, \hat{\alpha}_1, \hat{\alpha}_2, \ldots, \hat{\alpha}_k$ are the estimators of the structural parameters $\alpha_0, \alpha_1, \alpha_2, \ldots, \alpha_k$ of a particular regression model. The error term E in Eq. (A1) is replaced by its

estimator $\hat{E}$. Throughout this paper, the variance of the error term $\hat{E}$ is denoted by MSE (mean squared error, Appendix 3) [90].

2. The consistency assumption for considered models

This paper assumes that every theoretical point in the sample of $N = 23$ models is estimated consistently, that is without any bias, at least asymptotically. Therefore, every theoretical point on the scatter diagram coincides with the estimate obtained for n of hypothetical experiments testing this model. It follows that in the limits $n \to \infty$ and for all the population of models, the finite sample error $\hat{E}$ tends to E. Therefore, the requirement to use the method is the assumption that it is possible to determine the values of the estimators' model parameters from the experiment. Each model introduced into the analysis satisfies as many experimental constraints as possible. This group is referred to as an optimal sample of models in this paper.

3. The characteristics of the regressions

The total sum of squares (SS) of the dependent variable Y, $\text{SS}Y \equiv \text{SS}(Y) = \sum_{i=1}^{N} (Y_i - \overline{Y})^2$, is the sum of squares of deviations of the observed Y_i from their mean $\overline{Y}$. $\text{SS}(Y)$ can be partitioned to the sum of squares due to regression, $\text{SSR} = \sum_{i=1}^{N} (\widehat{Y}_i - \overline{Y})^2$, and due to error, $\text{SSE} = \sum_{i=1}^{N} (Y_i - \widehat{Y}_i)^2$, where SSE is called the residual (error) sum of squares. Thus, the analysis of variance (ANOVA) equation for the linear regression, $\text{SS}Y = \text{SSR} + \text{SSE}$, is valid [90]. The characteristics of the regressions used are also the mean square due to regression $\text{MSR} = \text{SSR}/df_{\text{SSR}}$, the mean squared error $\text{MSE} = \text{SSE}/df_{\text{SSE}}$ (the variance of the error term $\hat{E}$), and the coefficient of determination $R^2 = \text{SSR}/\text{SS}Y \in \langle 0, 1 \rangle$. Here, $df_{\text{SSR}} = k$ and $df_{\text{SSE}} = N - k - 1$ are the numbers of degrees of freedom of SSR and SSE, respectively. The descriptive limits of the correlation strength in the paper were assumed to be $0.1 < R^2 < 0.25$ for weak correlation and $R^2 \geqslant 0.64$ ($|R| \geqslant 0.8$) for strong correlation. In the case of one-dimensional linear regression, $Y = a + bX + \hat{E}$, the sign of the (Pearson) linear correlation coefficient r_{YX} between Y and X [90] agrees with the sign of b, i.e., $r_{YX} = \text{sgn}(b)\,|R|$.

Given a linear regression model, Eq. (A2), with k factors, the null hypothesis

$$H_0 : \alpha_1 = \alpha_2 = \cdots = \alpha_k = 0 \tag{A5}$$

is a question about the irrelevance of the correlation between the dependant variable Y and the group of explanatory variables X_i, $i = 1, 2, \ldots, k$. Suppose the null hypothesis H_0 is true. In that case, the test statistics $F = \text{MSR}/\text{MSE}$, which is the random variable on the sample space, has the F distribution $F_{k,N-k-1}$ with the number of degrees of freedom of the numerator $df_{\text{SSR}} = k$ and denominator $df_{\text{SSE}} = N - k - 1$. The method used to verify the hypothesis H_0 consists in calculating the value of the F statistic based on an observed sample denoted by F_{obs}. Thus, F_{obs} is the observed value of the F statistics in the sample of $N = 23$ examined models (or in groups I, II, and III). The empirical significance level, the so-called p value, is defined as the probability

$p = \text{Prob}(F \geqslant F_{\text{obs}})$. If $p > \alpha$, where α is the chosen significance level (e.g., 0.05 or 0.1), the regression is considered statistically insignificant. If $p \leqslant \alpha$, then the null hypothesis (A5) is rejected, and the conclusion is that there is a significant relationship between the set of independent variables $X_1, X_2, \ldots X_k$ and the dependent variable Y.

4. Type I and II sums of squares

In this paper the possible interaction terms between factors are neglected. If the maximal model includes $k' = 3$ factors X_1, X_2, and X_3, then $\text{SSE}_{k'} \equiv \text{SSE}(X_1, X_2, X_3)$ can be calculated. The lower models with $k = 2$ factors are treated similarly, i.e., $\text{SSE}_k = \text{SSE}(X_1, X_2)$. The impact of a particular factor can be tested by examining the SS differences. For example, to determine the significance of X_3, the partial F_{p} statistics for the models (X_1, X_2, X_3) and (X_1, X_2) can be calculated [90]:

$$F_{\text{p}} = \frac{(\text{SSE}_k - \text{SSE}_{k'})/(df_{\text{SSR},k'} - df_{\text{SSR},k})}{\text{MSE}_{k'}}. \quad (A6)$$

The statistics F_{p} is a random variable on the sample space, having the F distribution $F_{k'-k, N-k'-1}$ with the number of degrees of freedom of the numerator equal to $df_{\text{SSR},k'} - df_{\text{SSR},k} = k' - k$ and of the denominator equal to $df_{\text{SSE},k'} = N - k' - 1$ (see Appendix 3). For a particular sample, F_{p} takes the observed value F_p^{obs}. In this case, the p value can be calculated:

$$p = \text{Prob}\left(F_{\text{p}} \geqslant F_{\text{p}}^{\text{obs}}\right). \quad (A7)$$

If in the observed sample, for a chosen significance level α, $p > \alpha$, then there is no reason to reject the null hypothesis H_0, which now reads, "the lower model fits the observed data as well as the higher model." This means no hints are coming from the sample to extend the model. The lower model is rejected if $p \leqslant \alpha$. With the hierarchical development of the regression model, the value of the partial statistics F_{p} in the observed sample and the corresponding p values [Eq. (A7)] for the factors added last can be determined at all stages of model construction.

The different types of sum of squares are used depending on the model building procedure; among others, type I and II SS are of value [90].

The type I SS is defined as the difference in the sum of squares and is often called the sequential sum of squares. Initially, while building a model for the dependent variable Y, the only variable by the free term (intercept) in the regression model is a constant, denoted here by I. At this stage, if a variable X_1 has the largest value of R^2, it can be added to the model. The so extended model with added variable X_1 has $k' = 1$. Beginning the regression analysis with the single nontrivial independent variable X_1, the F_{p} test for the hypothesis that there is a fit to the sample in the intercept-only regression model coincides with the nonsignificance test for the slope coefficient, standing by the variable X_1 [90]. Subsequently, if an additional factor X_2 is needed, it must have the highest value of F_{p} at this stage, and so on. Type I SS is now $\text{SS}(X_2|X_1) = \text{SSE}(X_1) - \text{SSE}(X_1, X_2) = \text{SSR}(X_1, X_2) -$

$\text{SSR}(X_1)$, which is the sum of squares for the X_2 factor after the X_1 factor is taken into account. The F_{p} test coincides with the test for the statistical non-significance of the slope coefficient standing in the regression model next to the independent variable X_2, which was added at this stage. Subsequently, type I SS of $\text{SS}(X_3|X_1, X_2) = \text{SSE}(X_1, X_2) - SSE(X_1, X_2, X_3) = \text{SSR}(X_1, X_2, X_3) - \text{SSR}(X_1, X_2)$, which is in the numerator of F_{p} for $k' = 3$ and $k = 2$, Eq. (A6), is calculated. It gives the sum of squares for X_3 factor after two factors X_1 and X_2 are taken into account. Although the main tool in extending the model is type I SS, it is informative to check whether all the variables in the model are statistically significant after constructing the model that is accepted as the maximal one. Therefore, type II SS, which comes down to calculating $\text{SS}(\text{one of the considered variables} \,|\, \text{other variables})$ is used to check the loss in the fit due to the removal of the particular variable from the maximal model [90].

For the purpose of the analysis presented in Secs. IV B 1 and IV B 2, type I SS and type II SS are calculated for the dependent variable $n_{t,2}$ and the following factors in the model hierarchy: $(P_{t,2})$, $(P_{t,2}, L_{\text{sym},2})$, and $(P_{t,2}, L_{\text{sym},2}, K_{\text{sym},2})$. The same analysis is also performed for factors $P_{t,24}$, $L_{\text{sym},24}$, $K_{\text{sym},24}$ and the dependent variable $n_{t,24}$ (see Table XIII).

5. The stability of estimators of structural parameters

The primary indicator of the strength of the correlation between two independent variables X and Z is Pearson's linear correlation coefficient squared $R_X^2 \equiv R^2 = r_{XZ}^2$ (Appendix 3) with X being the selected (reference) factor. Based on the value of R_X^2, the variance inflation factor can be introduced [90]:

$$\text{VIF}_X = \frac{1}{1 - R_X^2}. \quad (A8)$$

If $\text{VIF}_X = 1$ the variables X and Z are not correlated. In accord to ranges of values of R^2, the variables are moderately correlated if $\text{VIF}_X \in (1.3, 2.8)$. High collinearity in the sample is understood if $\text{VIF}_X \geqslant 2.8$. It is customary to assume that if $\text{VIF}_X > 10$, which corresponds to $R_X^2 > 0.9$, then X should be removed from the group of factors [90]. The reason for removing factors with too large VIF_X is as follows. It can be shown that the estimator $\widehat{\sigma^2}_{\hat{\alpha}_X}$ of the variance $\sigma_{\hat{\alpha}_X}^2$ of the estimator $\hat{\alpha}_X$ of the structural parameter α_X in the $Y = \alpha_0 + \alpha_X X + \alpha_Z Z + E$ regression model has the following form [90]:

$$\widehat{\sigma^2}_{\hat{\alpha}_X} = c_X \, \text{VIF}_X, \quad (A9)$$

where the corresponding coefficient c_X depends on the data [90]. Therefore, removing the independent variable X, which has too big VIF_X, leads to a regression model for the dependent variable Y, which could be reliably used in another sample of models.

In the case of more factors, the square of the multiple correlation coefficient R_X^2 is determined between the selected factor X and the group of other independent variables [90]. In

TABLE XIII. Type I SS and type II SS for $Y \equiv n_t$ with factors in the model hierarchy (P_t), (P_t, L_{sym}) and maximal model $(P_t, L_{\mathrm{sym}}, K_{\mathrm{sym}})$, for the parabolic (index 2) and fourth-order (index 24) approximations. I [e.g., in SSE(I)] denotes a constant variable standing by the intercept coefficient. The analysis is performed for all groups.

Parabolic approximation			
SSE(I) = SSY	SSE$(I, P_{t,2})$	SSE$(I, P_{t,2}, L_{\mathrm{sym},2})$	SSE$(I, P_{t,2}, L_{\mathrm{sym},2}, K_{\mathrm{sym},2})$
0.00052462	0.00040207	0.00008523	0.00002525
SSR(I)	SSR$(I, P_{t,2})$	SSR$(I, P_{t,2}, L_{\mathrm{sym},2})$	SSR$(I, P_{t,2}, L_{\mathrm{sym},2}, K_{\mathrm{sym},2})$
0	0.00012255	0.00043939	0.00049937
Type I SS	Type I SS	Type I SS	
SS$(P_{t,2}\|I)$	SS$(L_{\mathrm{sym},2}\|I, P_{t,2})$	SS$(K_{\mathrm{sym},2}\|I, P_{t,2}, L_{\mathrm{sym},2})$	SS$(P_{t,2}\|I)$
= SSE(I) − SSE$(I, P_{t,2})$	= SSE$(I, P_{t,2})$ − SSE$(I, P_{t,2}, L_{\mathrm{sym},2})$	= SSE$(I, P_{t,2}, L_{\mathrm{sym},2})$	+SS$(L_{\mathrm{sym},2}\|I, P_{t,2})$
= SSR$(I, P_{t,2})$ − SSR(I)	= SSR$(I, P_{t,2}, L_{\mathrm{sym},2})$ − SSR$(I, P_{t,2})$	−SSE$(I, P_{t,2}, L_{\mathrm{sym},2}, K_{\mathrm{sym},2})$	+SS$(K_{\mathrm{sym},2}\|I, P_{t,2}, L_{\mathrm{sym},2})$
		= SSR$(I, P_{t,2}, L_{\mathrm{sym},2}, K_{\mathrm{sym},2})$	= SSR$(I, P_{t,2}, L_{\mathrm{sym},2}, K_{\mathrm{sym},2})$
		−SSR$(I, P_{t,2}, L_{\mathrm{sym},2})$	
0.00012255	0.00031684	0.00005999	
	Type II SS	Type II SS	Type II SS
	SS$(K_{\mathrm{sym},2}\|I, P_{t,2}, L_{\mathrm{sym},2})$	SS$(P_{t,2}\|I, L_{\mathrm{sym},2}, K_{\mathrm{sym},2})$	SS$(L_{\mathrm{sym},2}\|I, P_{t,2}, K_{\mathrm{sym},2})$
	= SSE$(I, P_{t,2}, L_{\mathrm{sym},2})$	= SSE$(I, L_{\mathrm{sym},2}, K_{\mathrm{sym},2})$	= SSE$(I, P_{t,2}, K_{\mathrm{sym},2})$
	−SSE$(I, P_{t,2}, L_{\mathrm{sym},2}, K_{\mathrm{sym},2})$	−SSE$(I, L_{\mathrm{sym},2}, K_{\mathrm{sym},2}, P_{t,2})$	−SSE$(I, P_{t,2}, K_{\mathrm{sym},2}, L_{\mathrm{sym},2})$
	0.00005999	0.00046043	0.00037434

Fourth-order approximation			
SSE(I) = SSY	SSE$(I, P_{t,2})$	SSE$(I, P_{t,24}, L_{\mathrm{sym},24})$	SSE$(I, P_{t,24}, L_{\mathrm{sym},24}, K_{\mathrm{sym},24})$
0.0005728	0.00049861	8.39083×10^{-5}	2.63879×10^{-5}
SSR(I)	SSR$(I, P_{t,24})$	SSR$(I, P_{t,24}, L_{\mathrm{sym},24})$	SSR$(I, P_{t,24}, L_{\mathrm{sym},24}, K_{\mathrm{sym},24})$
0	7.4197×10^{-5}	0.0004889	0.00054642
Type I SS	Type I SS	Type I SS	
SS$(P_{t,24}\|I)$	SS$(L_{\mathrm{sym},24}\|I, P_{t,24})$	SS$(K_{\mathrm{sym},24}\|I, P_{t,24}, L_{\mathrm{sym},24})$	SS$(P_{t,24}\|I)$
= SSE(I) − SSE$(I, P_{t,24})$	= SSE$(I, P_{t,24})$ − SSE$(I, P_{t,24}, L_{\mathrm{sym},24})$	= SSE$(I, P_{t,24}, L_{\mathrm{sym},24})$	+SS$(L_{\mathrm{sym},24}\|I, P_{t,24})$
= SSR$(I, P_{t,24})$ − SSR(I)	= SSR$(I, P_{t,24}, L_{\mathrm{sym},24})$ − SSR$(I, P_{t,24})$	−SSE$(I, P_{t,24}, L_{\mathrm{sym},24}, K_{\mathrm{sym},24})$	+SS$(K_{\mathrm{sym},24}\|I, P_{t,24}, L_{\mathrm{sym},24})$
		= SSR$(I, P_{t,24}, L_{\mathrm{sym},24}, K_{\mathrm{sym},24})$	= SSR$(I, P_{t,24}, L_{\mathrm{sym},24}, K_{\mathrm{sym},24})$
		−SSR$(I, P_{t,24}, L_{\mathrm{sym},24})$	
7.4197×10^{-5}	0.0004147	5.75205×10^{-5}	
	Type II SS	Type II SS	Type II SS
	SS$(K_{\mathrm{sym},24}\|I, P_{t,24}, L_{\mathrm{sym},24})$	SS$(P_{t,24}\|I, L_{\mathrm{sym},24}, K_{\mathrm{sym},24})$	SS$(L_{\mathrm{sym},24}\|I, P_{t,24}, K_{\mathrm{sym},24})$
	= SSE$(I, P_{t,24}, L_{\mathrm{sym},24})$	= SSE$(I, L_{\mathrm{sym},24}, K_{\mathrm{sym},24})$	= SSE$(I, P_{t,24}, K_{\mathrm{sym},24})$
	−SSE$(I, P_{t,24}, L_{\mathrm{sym},24}, K_{\mathrm{sym},24})$	−SSE$(I, L_{\mathrm{sym},24}, K_{\mathrm{sym},24}, P_{t,24})$	−SSE$(I, P_{t,24}, K_{\mathrm{sym},24}, L_{\mathrm{sym},24})$
	0.00005752	0.00043753	0.00045592

this sense, the variance inflation factor measures the amount of multicollinearity in regression analysis.

6. Partial and multiple correlations

A notorious problem in data analysis is avoiding spurious correlations caused, e.g., by the amplified or masking effect of other variables. To this aim, partial correlation analysis is often helpful. The main tool is the first-order partial correlation coefficient $r_{YX|Z}$ between, presumably linearly related to Z, variables X and Y, adjusted for the variable Z [90,91]:

$$r_{YX|Z} = \frac{r_{YX} - r_{YZ}\, r_{XZ}}{\sqrt{1 - r_{YZ}^2}\sqrt{1 - r_{XZ}^2}}. \qquad (A10)$$

It measures the strength and direction of the linear relationship between two variables Y and X after the effect of the variable Z is under control, and obviously, $r_{YX|Z} \in \langle -1, 1 \rangle$. The square of the partial correlation coefficient $r_{YX|Z}$ can take the form

$$r_{YX|Z}^2 = \frac{\mathrm{SSE}(Z) - \mathrm{SSE}(X, Z)}{\mathrm{SSE}(Z)}, \qquad (A11)$$

and thus measures the proportion of the residual sum of squares that is accounted for by adding X to a regression model already involving Z. It can be shown that the partial correlation coefficient $r_{YX|Z}$ equals the correlation of the residuals of the linear regression of Y vs Z and of X vs Z, i.e.,

$$r_{YX|Z} = r_{Y-\hat{Y}, X-\hat{X}}. \qquad (A12)$$

If $|r_{YX|Z}| < |r_{YX}|$, the variable Z is referred to as a confounder, and if $|r_{YX|Z}| > |r_{YX}|$, the variable Z is often called a mediator. In the case of Z being a mediator, the partial correlation between X and Y with Z being under control is interpreted as a direct influence of X on Y.

To measure associations linked to multiple regression, one introduces the multiple correlation coefficient. It describes the linear relationship between a dependent variable Y and several independent variables. Considering two independent variables

X and Z, the multiple correlation coefficient $R_{Y|ZX} = R_{Y|XZ} \in \langle 0, 1 \rangle$ is given by

$$R_{Y|XZ} = \sqrt{1 - \left(1 - r_{YX}^2\right)\left(1 - r_{YZ|X}^2\right)}. \qquad (A13)$$

In the case of three different independent variables X, Z, and W, the multiple correlation coefficient $R_{Y|XZW} \in \langle 0, 1 \rangle$ is given by the formula

$$R_{Y|XZW} = \sqrt{1 - \left(1 - r_{YX}^2\right)\left(1 - r_{YZ|X}^2\right)\left(1 - r_{YW|XZ}^2\right)}, \qquad (A14)$$

where $r_{YW|XZ} = r_{YW|ZX}$ is the second-order partial correlation coefficient [90]:

$$r_{YW|XZ} = \frac{r_{YW|X} - r_{YZ|X}\, r_{WZ|X}}{\sqrt{1 - r_{YZ|X}^2}\sqrt{1 - r_{WZ|X}^2}}. \qquad (A15)$$

The coefficient $r_{YW|XZ} \in \langle -1, 1 \rangle$ is the measure of the correlation between Y and W with the variables X and Z under control.

---

[1] N. K. Glendenning, *Compact Stars: Nuclear Physics, Particle Physics, and General Relativity* (Springer, New York, 1997).

[2] F. Weber, *Pulsars as Astrophysical Laboratories for Nuclear and Particle Physics* (Institute of Physics, Bristol, 1999).

[3] J. M. Lattimer and M. Prakash, Science **304**, 536 (2004).

[4] A. W. Steiner, M. Prakash, J. M. Lattimer, and P. J. Ellis, Phys. Rep. **411**, 325 (2005).

[5] P. Haensel, A. Potekhin, and D. Yakovlev, *Neutron Stars 1: Equation of State and Structure* (Springer, Berlin, 2007).

[6] M. Baldo and G. F. Burgio, Prog. Part. Nucl. Phys. **91**, 203 (2016).

[7] M. Oertel, M. Hempel, T. Klähn, and S. Typel, Rev. Mod. Phys. **89**, 015007 (2017).

[8] J. W. Holt and Y. Lim, Phys. Lett. B **784**, 77 (2018); S. S. Avancini, L. Brito, J. R. Marinelli, D. P. Menezes, M. M. W. de Moraes, C. Providência, and A. M. Santos, Phys. Rev. C **79**, 035804 (2009).

[9] V. Baran, M. Colonna, V. Greco, and M. Di Toro, Phys. Rep. **410**, 335 (2005).

[10] F. S. Zhang and L. W. Chen, Chin. Phys. Lett. **18**, 142 (2001).

[11] A. W. Steiner, Phys. Rev. C **74**, 045808 (2006).

[12] J. Xu, L.-W. Chen, B.-A. Li, and H.-R. Ma, Astrophys. J. **697**, 1549 (2009).

[13] W. M. Seif and D. N. Basu, Phys. Rev. C **89**, 028801 (2014).

[14] B.-A. Li, P. G. Krastev, D.-H. Wen, and N.-B. Zhang, Eur. Phys. J. A **55**, 117 (2019).

[15] I. Bednarek, J. Sładkowski, and J. Syska, J. Phys. Soc. Jpn. **88**, 124201 (2019).

[16] I. Bednarek, J. Sładkowski, and J. Syska, Symmetry **12**, 898 (2020).

[17] R. Wang and L.-w. Chen, Phys. Lett. B **773**, 62 (2017).

[18] B. J. Cai and L. W. Chen, Phys. Rev. C **85**, 024302 (2012).

[19] J. Pu, Z. Zhang, and L.-W. Chen, Phys. Rev. C **96**, 054311 (2017).

[20] N. Kaiser, Phys. Rev. C **91**, 065201 (2015).

[21] Z. W. Liu, Z. Qian, R. Y. Xing, J. R. Niu, and B. Y. Sun, Phys. Rev. C **97**, 025801 (2018).

[22] R. Nandi and S. Schramm, Phys. Rev. C **94**, 025806 (2016).

[23] B.-J. Cai and B.-A. Li, Phys. Rev. C **92**, 011601(R) (2015).

[24] B.-J. Cai and B.-A. Li, Phys. Rev. C **93**, 014619 (2016).

[25] O. Hen, B. A. Li, W. J. Guo, L. B. Weinstein, and E. Piasetzky, Phys. Rev. C **91**, 025803 (2015).

[26] C. J. Horowitz, E. F. Brown, Y. Kim, W. G. Lynch, R. Michaels, A. Ono, J. Piekarewicz, M. B. Tsang, and H. H. Wolter, J. Phys. G: Nucl. Part. Phys. **41**, 093001 (2014).

[27] Y. Zhang, P. Danielewicz, M. Famiano, Z. Li, W. G. Lynch, and M. B. Tsang, Phys. Lett. B **664**, 145 (2008).

[28] M. Zielinska-Pfabe, Acta Phys. Pol. B Proc. Suppl. **10**, 153 (2017).

[29] J. M. Pearson, N. Chamel, A. F. Fantina, and S. Goriely, Eur. Phys. J. A **50**, 43 (2014).

[30] D. Adhikari *et al.* (PREX Collaboration), Phys. Rev. Lett. **126**, 172502 (2021).

[31] T.-G. Yue, L.-W. Chen, Z. Zhang, and Y. Zhou, Phys. Rev. Res. **4**, L022054 (2022).

[32] L.-W. Chen, Ch. M. Ko, and B.-A. Li, Phys. Rev. C **72**, 064309 (2005).

[33] Z. Z. Li, Y. F. Niu, and W. H. Long, Phys. Rev. C **103**, 064301 (2021).

[34] V. Baran, M. Colonna, M. Di Toro, A. Croitoru, and D. Dumitru, Phys. Rev. C **88**, 044610 (2013).

[35] P. Danielewicz and J. Lee, Nucl. Phys. A **922**, 1 (2014).

[36] M. B. Tsang, T. X. Liu, L. Shi, P. Danielewicz, C. K. Gelbke, X. D. Liu, W. G. Lynch, W. P. Tan, G. Verde, A. Wagner, H. S. Xu, W. A. Friedman, L. Beaulieu, B. Davin, R. T. de Souza, Y. Larochelle, T. Lefort, R. Yanez, V. E. Viola, Jr., R. J. Charity, and L. G. Sobotka, Phys. Rev. Lett. **92**, 062701 (2004).

[37] Z. Chen, S. Kowalski, M. Huang, R. Wada, T. Keutgen *et al.*, Phys. Rev. C **81**, 064613 (2010).

[38] J. Piekarewicz, Eur. Phys. J. A **50**, 25 (2014).

[39] X.-H. Li, B.-J. Cai, L.-W. Chen, R. Chen, and B.-A. Li, C. Xu, Phys. Lett. B **721**, 101 (2013).

[40] B.-A. Li, Nucl. Phys. News **27**, 7 (2017).

[41] D. Adhikari *et al.* (CREX Collaboration), Phys. Rev. Lett. **129**, 042501 (2022).

[42] B. T. Reed, F. J. Fattoyev, C. J. Horowitz, and J. Piekarewicz, Phys. Rev. Lett. **126**, 172503 (2021).

[43] R. Essick, I. Tews, P. Landry, and A. Schwenk, Phys. Rev. Lett. **127**, 192701 (2021).

[44] P. G. Reinhard, X. Roca-Maza, and W. Nazarewicz, Phys. Rev. Lett. **127**, 232501 (2021).

[45] C. Mondal and F. Gulminelli, Phys. Rev. C **107**, 015801 (2023).

[46] K. Tuchitani, Y. Horinouchi, K.-I. Makino, N. Noda, H. Kouno, T. Iwamitsu, M. Nakano, and A. Hasegawa, Int. J. Mod. Phys. E **14**, 955 (2005).

[47] B. D. Serot and J. D. Walecka, Adv. Nucl. Phys. **16**, 1 (1986).

[48] B. D. Serot and J. D. Walecka, Int. J. Mod. Phys. E **06**, 515 (1997).

[49] J. Boguta and A. R. Bodmer, Nucl. Phys. A **292**, 413 (1977).

[50] I. Bednarek, R. Manka, and M. Pienkos, PLoS ONE **9**, e106368 (2014).

[51] M. Dutra, O. Lourenço, S. S. Avancini, B. V. Carlson, A. Delfino, D. P. Menezes, C. Providência, S. Typel, and J. R. Stone, Phys. Rev. C **90**, 055203 (2014).

[52] M. Dutra, O. Lourenço, O. Hen, E. Piasetzky, and D. P. Menezes, Chin. Phys. C **42**, 064105 (2018).

[53] M. B. Tsang, Y. Zhang, P. Danielewicz, M. Famiano, Z. Li, W. G. Lynch, and A. W. Steiner, Phys. Rev. Lett. **102**, 122701 (2009).

[54] J. R. Stone and P. G. Reinhard, Prog. Part. Nucl. Phys. **58**, 587 (2007).

[55] M. B. Tsang, J. R. Stone, F. Camera, P. Danielewicz, S. Gandolfi, K. Hebeler, C. J. Horowitz, J. Lee, W. G. Lynch, Z. Kohley, R. Lemmon, P. Moller, T. Murakami, S. Riordan, X. Roca-Maza, F. Sammarruca, A. W. Steiner, I. Vidaña, and S. J. Yennello, Phys. Rev. C **86**, 015803 (2012).

[56] B.-A. Li *et al.*, J. Phys.: Conf. Ser. **312**, 042006 (2011).

[57] M. Centelles, X. Roca-Maza, X. Viñas, and M. Warda, Phys. Rev. Lett. **102**, 122502 (2009).

[58] T. Li, U. Gang, Y. Liu, R. Marks, B. K. Nayak, P. V. R. Madhusudhana, M. Fujiwara, H. Hashimoto, K. Kawase, K. Nakanishi, S. Okumura, M. Yosoi, M. Itoh, M. Ichikawa, R. Matsuo, T. Terazono, M. Uchida, T. Kawabata, H. Akimune, Y. Iwao, T. Murakami *et al.* Phys. Rev. Lett. **99**, 162503 (2007).

[59] P. Danielewicz, Nucl. Phys. A **727**, 233 (2003).

[60] T. Malik, M. Ferreira, M. B. Albino, and C. Providência, Phys. Rev. D **107**, 103018 (2023).

[61] S. Typel and H. H. Wolter, Nucl. Phys. A **656**, 331 (1999).

[62] B. G. Todd-Rutel and J. Piekarewicz, Phys. Rev. Lett. **95**, 122501 (2005).

[63] S. Shlomo, V. M. Kolomietz, and G. Col'o, Eur. Phys. J. A **30**, 23 (2006).

[64] R. Essick, P. Landry, A. Schwenk, and I. Tews, Phys. Rev. C **104**, 065804 (2021).

[65] K. Hebeler, J. M. Lattimer, C. J. Pethick, and A. Schwenk, Astrophys. J. **773**, 11 (2013).

[66] E. Fonseca *et al.*, Astrophys. J. Lett. **915**, L12 (2021).

[67] S. K. Dhiman, R. Kumar, and B. K. Agrawal, Phys. Rev. C **76**, 045801 (2007).

[68] R. Kumar, B. K. Agrawal, and S. K. Dhiman, Phys. Rev. C **74**, 034323 (2006).

[69] B. K. Agrawal, Phys. Rev. C **81**, 034323 (2010).

[70] R. J. Furnstahl, B. D. Serot, and H. B. Tang, Nucl. Phys. A **615**, 441 (1997).

[71] A. Sulaksono and T. Mart, Phys. Rev. C **74**, 045806 (2006).

[72] J. Piekarewicz and S. P. Weppner, Nucl. Phys. A **778**, 10 (2006).

[73] F. J. Fattoyev, C. J. Horowitz, J. Piekarewicz, and G. Shen, Phys. Rev. C **82**, 055803 (2010).

[74] Y. Sugahara and H. Toki, Nucl. Phys. A **579**, 557 (1994).

[75] I. Bednarek, W. Olchawa, J. Sladkowski, and J. Syska, Phys. Rev. C **106**, 055805 (2022).

[76] C. Providência, L. Brito, S. S. Avancini, D. P. Menezes, and Ph. Chomaz, Phys. Rev. C **73**, 025805 (2006).

[77] C. Ducoin, C. Providência, A. M. Santos, L. Brito, and Ph. Chomaz, Phys. Rev. C **78**, 055801 (2008).

[78] S. S. Avancini, S. Chiacchiera, D. P. Menezes, and C. Providência, Phys. Rev. C **82**, 055807 (2010).

[79] S. S. Avancini, S. Chiacchiera, D. P. Menezes, and C. Providência, Phys. Rev. C **85**, 059904(E) (2012).

[80] S. Kubis, Phys. Rev. C **70**, 065804 (2004).

[81] S. Kubis, Phys. Rev. C **76**, 025801 (2007).

[82] J. M. Lattimer and M. Prakash, Phys. Rep. **442**, 109 (2007).

[83] J. Xu, L. W. Chen, B. A. Li, and H. R. Ma, Phys. Rev. C **79**, 035802 (2009).

[84] P. Char, Ch. Mondal, F. Gulminelli, and M. Oertel, arXiv:2307.12364.

[85] I. Vidaña, C. Providência, A. Polls, and A. Rios, Phys. Rev. C **80**, 045806 (2009).

[86] C. Providência, S. S. Avancini, R. Cavagnoli, S. Chiacchiera, C. Ducoin, F. Grill, J. Margueron, D. P. Menezes, A. Rabhi, and I. Vidaña, Eur. Phys. J. A **50**, 44 (2014).

[87] I. Tews, J. M. Lattimer, A. Ohnishi, and E. E. Kolomeitsev, Astrophys. J. **848**, 105 (2017).

[88] N. Alam, B. K. Agrawal, M. Fortin, H. Pais, C. Providência, Ad. R. Raduta, and A. Sulaksono, Phys. Rev. C **94**, 052801(R) (2016).

[89] C. Ducoin, J. Margueron, C. Providência, and I. Vidaña, Phys. Rev. C **83**, 045810 (2011).

[90] D. G. Kleinbaum, L. L. Kupper, K. E. Muller, and A. Nizam, *Applied Regression Analysis and Other Multivariable Method* (Cengage Learning, Boston, 2014).

[91] M. G. Kendall, *The Advanced Theory of Statistics* (Charles Griffin & Company, London, 1945), Vol. 1.

[92] S. Wright, J. Agric. Res. **20**, 557 (1921).

[93] D. F. Alwin and R. M. Hauser, Am. Sociol. Rev. **40**, 37 (1975).

[94] W. G. Newton, M. Gearheart, and B.-A. Li, Astrophys. J. Suppl. Series **204**, 9 (2013).

[95] H. Pais and C. Providência, Phys. Rev. C **94**, 015808 (2016).

[96] H. Pais, B. Bertolino, J. Fang, X. Wang, and C. Providência, Eur. Phys. J. A **57**, 193 (2021).